

**The Virtual Seismologist (VS) method: a Bayesian approach to earthquake early
warning**

by

Georgia Cua¹, Thomas Heaton²

1. Puerto Rico Seismic Network, Univeristy of Puerto Rico Mayagüez, Puerto Rico,
USA.
2. Department of Civil Engineering, California Institute of Technology, Pasadena, USA.

1. Introduction

Subscribers attempting to use early warning information to reduce earthquake-related losses typically have a selected sequence of actions they would like to complete before damaging ground motions reach their site. These subscribers decide whether or not to initiate their damage-mitigating actions based on uncertain information. How to make optimal decisions with uncertain information is a fundamental question to these subscribers. Answering this question properly requires addressing a seismological and an economics problem in tandem. The seismological question is that of real-time earthquake source estimation, which can be phrased as follows: what are the best estimates of magnitude and location given the available data? The economics question is the user response problem, which can be phrased as follows: what is the optimal decision or course of action, given the current source estimates and its uncertainties?

The Virtual Seismologist (VS) method is a Bayesian approach to earthquake early warning that addresses the source estimation and user response problems in tandem. In the source estimation problem, the VS method shares with other proposed methodologies (Nakamura, 1988; Allen and Kanamori, 2003; Wu and Kanamori, 2005a, 2005b) the use of relative frequency content or predominant period and attenuation relationships to estimate magnitude and/or location from available ground motion observations. The introduction of prior information into the earthquake source estimation problem distinguishes the VS method from other paradigms for early warning. Bayes' theorem allows the use of a "background" state of knowledge to help in resolving trade-offs in magnitude and location that cannot be resolved due to the scarcity of observations at the initial stages of the earthquake rupture. Types of information that can be included in the Bayes prior include: state of health of the seismic network, previously observed seismicity, known fault locations, and the Gutenberg-Richter magnitude-frequency relationship. The benefits of prior information are largest in regions with low station density, where large inter-station distances result in initial early warning estimates based on a sparse set of observations. We illustrate the performance of the VS method with high station density using ground motions recorded from the $M = 4.75$ Yorba Linda, California earthquake, and with low station density using data from the $M = 7.1$ Hector Mine, California earthquake. The examples shown in this paper approximate the earthquake as a single point source. While this seems adequate for earthquakes with $M < 6$, this methodology needs to be modified to be effective for long ruptures where near-source ground motions are expected even at large distance from the epicenter. Yamada and Heaton (2006) present a strategy for extending VS to handle long ruptures.

Aside from a method to estimate magnitude and location from sparse information from the initial stages of the earthquake rupture, it is equally important for earthquake early warning studies to address how subscribers might make optimal decisions using early warning information. Different subscribers will require different types of early warning estimates, depending on subscriber tolerance to missed and/or false alarms. Ultimately, the subscriber requirements dictate how the source estimation problem must be phrased.

This is not consistent with the traditional separation of the source estimation and user response problems in earthquake early warning research. The VS method facilitates an integrated approach that recognizes the role of the user decision-making process in formulating the source estimation problem.

2. Real-time earthquake source estimation

2.1 Review of Bayes' Theorem

Consider that we want to estimate the magnitude and location of an earthquake given an available set of observed ground motions. According to Bayes theorem, the state of belief regarding magnitude and location (M, loc) given a set of available observations Y_{obs} is given by

$$P(M, loc | Y_{obs}) = \frac{P(Y_{obs} | M, loc) \times P(M, loc)}{P(Y_{obs})} \quad (1)$$

where M is magnitude, loc is a location parameter (epicentral distance, or epicentral location), and Y_{obs} is the available set of observed ground motions. We can use the proportional form of Bayes' theorem since $P(Y_{obs})$ is not a function of the parameters being estimated (M, loc):

$$P(M, loc | Y_{obs}) \propto P(Y_{obs} | M, loc) \times P(M, loc) \quad (2)$$

$P(M, loc | Y_{obs})$, is the posterior probability density function (pdf); it is the conditional probability that an earthquake of magnitude and location M, loc generated the set of observations Y_{obs} . The VS estimates, $(M, loc)_{VS}$, are the most probable source estimates given the available observations; they maximize $P(M, loc | Y_{obs})$. The spread of $P(M, loc | Y_{obs})$ yields the uncertainties on the VS source estimates. On the right hand side, $P(Y_{obs} | M, loc)$ is the likelihood function; it is the conditional probability of observing a set of ground motions Y_{obs} given an earthquake with magnitude and location M, loc . The likelihood function requires ground motion models relating source descriptions (M, loc) to observed ground motion amplitudes. The VS method uses 1) relationships between ratios of peak ground motions and magnitude, and 2) ground motion attenuation relationships describing observed amplitudes as functions of magnitude and distance, to define the likelihood function $P(Y_{obs} | M, loc)$. $P(M, loc)$ is the Bayes prior; it represents a background state of knowledge, independent of the observations, on relative earthquake probabilities that we want to include in the estimation process. The degree of complexity that can be incorporated into the prior is flexible. The simplest prior we can use is the assumption that all magnitudes and all locations are equally probable. This simplifies the necessary calculations, at the cost of being an inaccurate representation of the general state of knowledge regarding earthquake occurrence. Alternatively, we could incorporate into the prior some generally accepted beliefs about earthquake occurrence: 1) the magnitude-frequency relationship of earthquakes follows the Gutenberg-Richter law, 2) many earthquakes occur on known faults, 3) and earthquakes often cluster in time and space. We can also include information about the state of health of the seismic network. The choice of prior information is most influential in the initial VS early warning estimates;

trade-offs between magnitude and location in the initial estimates are resolved in favor of the prior information. In real-time source estimation, the use of prior information is perhaps the most important distinction between the VS method and other proposed paradigms for early warning.

The evolution of VS early warning source estimates as a function of available information mimics how reasonable and educated humans (as opposed to unreasonable and prejudiced humans) modify their beliefs in light of new information. Early VS estimates are typically based on a scarce set of observations, for instance, on the first few seconds of peak amplitude data available at the first triggered station. In these early estimates, there will be trade-offs in magnitude and location that cannot be resolved by the available observations alone. At any given time, the VS estimates $(M, loc)_{VS}$ are the most probable source estimates; they maximize $P(M, loc | Y_{obs})$, and are consistent with the available observations, with trade-offs in magnitude and location resolved in favor of the given prior information. Initially, when observations are sparse, $(M, loc)_{VS}$ are strongly influenced by the prior; the observations become the dominant contributor as ground motions propagate to further stations. When sufficient observations are available to fully constrain the magnitude and location estimates, the choice of prior is irrelevant; $(M, loc)_{VS}$ are completely determined by the observations.

2.2 Defining the likelihood function, $P(Y_{obs}|M, loc)$

Let us initially assume a uniform prior, $P(M, loc) = c$, a constant. Eqn.(2) yields

$$P(M, loc | Y_{obs}) \propto P(Y_{obs} | M, loc) \quad (3)$$

Let Y_{obs} be the set of log peak acceleration, velocity, and filtered (3-second high pass) displacement on horizontal and vertical channels available at a given time. Assuming the Y_{obs} are independent and log normally distributed, maximizing $P(M, loc | Y_{obs})$ is equivalent to maximizing the log of the likelihood function, $L = \log(P(Y_{obs} | M, loc))$, which, for the most general case of P- and/or S-wave amplitudes available at multiple stations, we define as follows

$$L(Y_{obs}, M, loc) = \sum_{i=1}^n \sum_{j=1}^{P,S} L(M, loc)_{ij} \quad (4)$$

$$L(Y_{obs}, M, loc)_{ij} = \frac{(Z_{obs_{ij}} - \bar{Z}_j(M))^2}{2\sigma_Z^2} + \sum_{k=1}^4 \left(\frac{(Y_{obs_{ij}} - \bar{Y}_{ijk}(M, loc))^2}{2\sigma_{ijk}^2} \right) \quad (5)$$

$L(Y_{obs}, M, loc)$ incorporates 6 channels of ground motion (maximum vertical and maximum of 2 horizontal channels of acceleration, velocity, and filtered displacement) per station. We assume that each station has 1 vertical and 2 horizontal sensors with

acceleration or broadband velocity output, and that recursive filters can be used to provide acceleration, velocity, and filtered displacement in real-time. In Eqns. (4) and (5), i is an index over the n stations with P-wave triggers, j is an index over the P- and S-wave phases, and k is an index over observed vertical velocity, and horizontal acceleration, velocity, and filtered displacement, the channels that contribute to the likelihood function via ground motion attenuation relationships. The remaining two channels, observed vertical acceleration and filtered displacement, are accounted for by the term involving $Z_{obs_{ij}}$. $Z_{obs_{ij}}$ is the ratio of peak available vertical acceleration to peak available vertical filtered displacement found by Cua and Heaton (2006b) to be optimally indicative of magnitude; it is given by

$$Z_{obs_{ij}} = \log \left(\frac{PVA_{ij}^{0.36}}{PVD_{ij}^{0.93}} \right) = 0.36 \log(PVA_{ij}) - 0.93 \log(PVD_{ij}) \quad (6)$$

In Eqn.(6), PVA_{ij} and PVD_{ij} denote peak available vertical acceleration and peak vertical (filtered) displacement, respectively at the i^{th} station and for the j^{th} body wave. $Z_{obs_{ij}}$ is a measure of the relative frequency content of ground motion. Similar to methods based on predominant period (Nakamura, 1988; Allen and Kanamori, 2003; Wu and Kanamori, 2005ab), it is based on the idea that the relative frequency content of ground motions can be indicative of magnitude since small earthquakes involve small patches of slip and will radiate more high frequency energy, while large earthquakes involve finite rupture dimensions that contribute to longer period energy.

The details on the linear discriminant analysis used to determine $Z_{obs_{ij}}$ and its relationship to magnitude are found in Cua (2005) and Cua and Heaton (2006b). There are different coefficients characterizing the magnitude dependence of Z_{obs} (dropping the subscripts for brevity) for P- and S-waves.

$$\begin{aligned} \bar{Z}(M) &= -0.615M + 5.495, \quad \sigma_z = 0.17 \quad \text{for P-waves} \\ &= -0.685M + 5.517, \quad \sigma_z = 0.193 \quad \text{for S-waves} \end{aligned} \quad (7)$$

To use Eqns.(5), (6), and (7), it is necessary to estimate or assume whether the peak amplitudes at a given station are from a P- or S-wave. Cua (2005) and Cua and Heaton (2006b) developed the following criteria to distinguish between P- and S-waves

$$\begin{aligned} PS &= 0.43 \log(PVA) + 0.55 \log(PVV) - 0.46 \log(PHA) - 0.55 \log(PHV) \\ \text{if } PS > 0, & \text{ amplitudes are most likely from a P-wave} \\ \text{if } PS < 0, & \text{ amplitudes are most likely from an S-wave} \end{aligned} \quad (8)$$

In Eqn.(8), PVA denotes peak vertical acceleration, PVV peak vertical velocity, PHA peak horizontal acceleration, and PHV peak horizontal velocity. This criteria correctly identified P-waves 88% of the time in a database of ground motions from 70 Southern California earthquakes with $2 \leq M \leq 7.3$, and epicentral distances $R < 200$ km . Figure 1

shows magnitude against Z_{obs} from peak P-wave amplitudes from this dataset. Cua and Heaton (2006a) also used this database to develop the P- and S-wave amplitude attenuation relationships $\bar{Y}_{ijk}(M, R)$, which define the second term of the likelihood function.

The second term of the likelihood function represents the contribution of observed peak vertical velocity, peak horizontal acceleration, velocity, and displacement and their respective attenuation relationships $\bar{Y}_{ijk}(M, R)$ in constraining both magnitude and location. Eqn.(5) is expressed in terms of the source parameters M, loc ; in the most general case, loc represents the epicentral latitude and longitude coordinates. Given, epicentral latitude and longitude coordinates, the epicentral distance R can be calculated. Thus, $\bar{Y}_{ijk}(M, loc)$ is equivalent to $\bar{Y}_{ijk}(M, R)$, which Cua and Heaton (2006a) modeled as

$$\bar{Y}_{ijk}(M, R) = a_{jk}M - b_{jk}(R_{i_i} + C_{jk}(M)) - d_{jk} \log(R_{i_i} + C_{jk}(M)) + e_{jk} + \alpha_{ijk}$$

where $R_{i_i} = \sqrt{R_i^2 + 9}$, where R_i is the epicentral distance of the i^{th} station (9)

and $C_{jk}(M) = c_{1jk}(\arctan(M - 5) + \frac{\pi}{2}) \times \exp(c_{2jk}(M - 5))$

In VS method, the regression coefficients (a, b, c_1, c_2, d, e) - dropping the subscripts - are known quantities (Table 1). There are different sets of regression coefficients for different channels of ground motion, for P- and S-waves, and for rock and soil sites. The station-specific site correction factors α_{ijk} take into account systematic amplification or deamplification of ground motions observed at a given site relative to the mean ground motion levels predicted by the attenuation relationships. Cua and Heaton (2006b) determined α_{ijk} for 135 SCSN stations for horizontal and vertical acceleration, velocity, and filtered displacement; these are available online at <http://resolver.caltech.edu/CaltechETD:etd-02092005-125601>.

The VS source estimates, $(M, loc)_{VS}$, are the source parameters that maximize the posterior pdf $P(M, loc | Y_{obs})$; in general, these estimates are a function of prior information and the available observations. Let $(M, loc)_L$ refer to the source parameters that maximize the log likelihood, $L = \log(P(Y_{obs} | M, loc))$; these are the source estimates most consistent with the available observations, whether data is available at single or multiple stations. A single-station estimate involves setting $n = 1$ and, if desired, using epicentral distance R as the loc parameter. With a uniform prior, $(M, loc)_{VS} = (M, loc)_L$. The VS method requires a minimum of 3 seconds of data following the P- arrival (or 2 seconds of data following the S-arrival) before a station contributes its amplitudes to the likelihood function. It is assumed that P-waves can be detected via short-term over long-term average methods. The S-wave arrival can be determined using Eqn.(8).

The $(M, loc)_L$ at any given time is the point source that best fits (in a least squares sense) the geographical distribution of observed P- and S-wave amplitudes and ground motion ratios. The location estimate from the likelihood function is an amplitude-based location; no arrival time information or velocity structure is included. It is comparable to the strong motion centroid (Kanamori, 1993). Amplitude-based locations, while not very accurate, are more robust than locations based on phase arrivals, and are an efficient means to convey the spatial distribution of ground motion observations post-earthquake response (Kanamori, 1993). The likelihood function develops a global maximum as the ground motions propagate to further stations. In the early stages of the estimation process, when the set of available observations is sparse (for instance, 3 seconds after the initial P detection at the first triggered station), the likelihood function may not have a global maximum; there are trade-offs between the source estimates (a small earthquake located close by, or a larger event further away) that may be unresolved by the available observations. The inclusion of prior information is most useful in these situations.

2.3 *Defining the prior, $P(M, loc)$*

The Bayes prior is a statement of “background” knowledge relevant to the parameter estimation problem at hand. In the VS method, we use $P(M, loc)$ to introduce information on relative earthquake probabilities and the state-of-health of the seismic network into the real-time source estimation problem. We enumerate the different types of information that can be included in the prior.

- Long-term national hazard maps, or known fault traces, are good candidates to include in the Bayes prior since faults that have generated large earthquakes in the past, such as the San Andreas fault system in California, or the Northern Anatolian fault in Turkey, are likely to generate large events in the future.
- The Gutenberg-Richter law states that small events occur more frequently than large earthquakes. Short-term seismicity-based earthquake forecasts take into account that the magnitude-frequency distribution of earthquakes follows the Gutenberg-Richter law, and that earthquakes cluster in space and time, with Omori’s law governing the decay of number of aftershocks as a function of time after the mainshock (Reasenber and Jones, 1989; Gerstenberger, Wiemer, and Jones, 2003).
- The location of previously observed seismicity is important prior information since many large earthquakes have foreshocks. Abercrombie and Mori (1996) found that 44% of earthquakes in their dataset of 59 $M > 5$ California earthquakes had foreshocks. Jones (1984) found that 35% of earthquakes in a dataset of 20 San Andreas earthquakes had foreshocks within 1 day and 5 km of the mainshock.
- For a region with no known faults or previously observed seismicity, we can assume that all locations have equal probability of being an earthquake epicenter. This implies that epicentral distances are more likely to be larger than smaller.
- Nearest neighbor regions, or Voronoi cells, of operating stations provide useful constraints on earthquake locations. The Voronoi cell of a given station is the set of all location coordinates that are closer to the said station than any other station in the network. The initial P-wave detection from an event implies that the event nucleated within the Voronoi cell of the first triggered station. The denser the deployment of

stations within a seismic network, the smaller the area of the average station Voronoi cell, and the stronger the constraint on earthquake location.

- The concept of not-yet-arrived data, as described by Horiuchi et al (2004) and Rydelek and Pujol (2004), can be used along with station Voronoi cells to describe the evolution of regions of possible location following the initial P detection. In this article, we refer to the region consistent with observed arrivals as the region of possible location. It is independent of the amplitude-based location estimate obtained from maximizing the likelihood function. From Rydelek and Pujol (2004), the locations consistent with the first two P-arrivals satisfy

$$R_2 - R_1 = \bar{V}_P \times (t_2 - t_1) \quad (10)$$

where R_1 and R_2 are the respective epicentral distances of stations with the first 2 P-wave arrivals, t_1 and t_2 are the corresponding P-wave arrival times, and V_P is an average P-wave velocity. Given the time between the first 2 P detections, Eqn.(10) constrains the earthquake location to a hyperbola passing between the two stations.

As originally described by Horiuchi et al (2004) and Rydelek and Pujol (2004), not-yet-arrived data can be used once two P-wave detections are available. In contrast, Voronoi cells, in conjunction with a slightly modified use of not-yet-arrived data, can be used to describe continuously evolving constraints on earthquake locations even before the second P-wave arrival. Consider the following situation: there is an initial P-wave detection at station 1, and Δt seconds later, there are no subsequent P-wave detections at the m stations sharing a Voronoi edge with station 1. The non-arrivals at each of the $i = 1, K, m$ stations provide the inequality constraints

$$R_i - R_1 > \bar{V}_P \times \Delta t \quad (11)$$

The region of possible location is the intersection of the Voronoi cell of station 1 (constraint on location from the first P detection) and the areas consistent with the m inequality constraints described by Eqn.(11); the area of this region of possible location is inversely proportional to Δt . Once the P-wave arrives at the second closest station, the region of possible location collapses to the Rydelek and Pujol hyperbola. A third arrival locates the epicenter.

Voronoi cells are strictly prior information since they are derived from station locations, which are independent of the earthquake rupture process. In contrast, not-yet-arrived data is not strictly prior information, since the time elapsed since the initial P detection, Δt , is an observed quantity. However, we do not include Δt in the likelihood function since it does not involve observed amplitudes.

Prior information is particularly useful in regions with low station density, where time between the first and second P-wave detections may be relatively large.

3. Applications of the VS method to selected Southern California earthquake datasets

3.1 3 September 2002 $M=4.75$ Yorba Linda, California earthquake: high station density

The Yorba Linda earthquake occurred on 3 September 2002 in suburban Los Angeles, a region with a high density of real-time Southern California Seismic Network (SCSN) stations. The mainshock was located by SCSN at 33.92N, -117.78W, at a depth of 12.92 km (Hauksson et al, 2002). Two foreshocks (with magnitudes $M=2.66$ and $M=1.6$) occurred within 1 km of the mainshock epicenter in the 24 hours preceding the mainshock.

The application of the VS method illustrates how the approach works in regions with high station density. Station Voronoi cells, previously observed seismicity, and the Gutenberg-Richter relationships will be included in the Bayes prior, although the prior information is for the most part unnecessary. Due to the high station density in the epicentral region, there are quickly enough observations to constrain the source estimates without resort to prior information.

Figure 2 shows SCSN stations in the epicentral region. The triangles are the stations operational at the time of the mainshock; the polygons are the associated Voronoi cells. Circles are locations of $M > 1$ earthquakes recorded by SCSN in the 24 hours preceding the mainshock. Due to the high station density in this region, areas of Voronoi cells (those away from edges of the network) are relatively small, in the range of 250 to 700 km^2 . The initial arrival at station SRN constrains the location to the area within its Voronoi cell (shaded polygon). Figure 3 shows the relative probabilities of epicentral distances consistent with the initial arrival at SRN. One of the simplest assumptions we can make given an initial P detection is that the event is located at the first triggered station. From Figure 3, the largest possible error with this assumption is 15 km.

The initial VS estimate is based on peak amplitudes available 3 seconds after the initial P detection at station SRN. With data from a single station ($n = 1$ in Eqn.(4)), the source estimation problem can be parameterized in terms of magnitude and epicentral distance. Figure 4 shows contours of the likelihood function (no prior information) using peak amplitudes from 6 channels (horizontal and vertical acceleration, velocity, and filtered displacement) available at SRN 3 seconds after the initial P detection. The elongated contours of the likelihood function are indicative of trade-offs in magnitude and epicentral distance that are not fully resolved by the peak amplitudes at a single station. $M = 5.5$ and $R = 33$ km maximize the likelihood function. With the likelihood expressed in terms of M, R , we can include as prior information the range of epicentral distances consistent with the first arrival at SRN (Figure 3), as well as the Gutenberg-Richter relationship. Figure 5 shows the effects of including the Gutenberg-Richter relationship, in addition to the constraints on epicentral distance by the Voronoi cells, on contours of the posterior density function. Recall that the posterior pdf is the product of the likelihood and the prior pdfs, and that the source estimates that maximize the

posterior pdf are the most probable source estimates. $(M, R)_{VS}$, the most probable magnitude and epicentral distance estimates, are indicated in Figure 5. The 3-second VS estimates without the Gutenberg-Richter relationship in the prior are closer to the actual magnitude and epicentral distance obtained by using the SCSN arrival-based location than VS estimates including the Gutenberg-Richter relationship in the prior.

As the ground motions propagate to other stations, it is more convenient to parameterize the early warning location estimate in terms geographic coordinates (latitude, longitude) as opposed to epicentral distances of n stations. Figure 6 shows locations consistent with the 3-second peak amplitudes at SRN for different magnitude ranges. The trade-offs here are similar to those in Figure 4; we cannot unambiguously distinguish between small events in close and large events at distance using only amplitude information at a single station. The situation is much improved when previously observed seismicity and Voronoi cell constraints are taken into account. The best way to include previously observed seismicity into the estimation process would be to use short-term, seismicity-based earthquake forecasts such as STEP (Gerstenberger, Wiemer, Jones, 2003) as part of the prior. In this example, we simply increase the probability that a particular location is the event location by a factor of 2 if it is within 5 km of an event that occurred in the preceding 24 hours. Figure 7 shows contours of the posterior pdf (as a function of magnitude, latitude, and longitude) using peak amplitudes at SRN 3 seconds following the initial P detection to define the likelihood and including previously observed seismicity and the Voronoi cell information in the prior. The VS location estimate agrees with the SCSN location. The VS magnitude estimate without the Gutenberg-Richter relationship in the prior is $M = 4.8 \pm 0.4$, with the Gutenberg-Richter in the prior, it is $M = 4.4 \pm 0.4$. The SCSN-reported magnitude is $M = 4.75$.

Figure 8 shows the evolution of magnitude estimates as a function of duration of data from the seismic network. Estimates labeled “amplitudes only” maximize the likelihood function (no prior information). We distinguish between 2 VS magnitude estimates (both with station geometry and previously observed seismicity included in the prior) differing in whether or not the Gutenberg-Richter relationship was used in the prior. All magnitude estimates converge to the SCSN solution at large times, when there are sufficient available observations. The differences in the magnitude estimates in the earlier estimates are due to the differences in the prior information included. The VS estimate without the Gutenberg-Richter relationship is within 0.05 magnitude units of the SCSN-reported magnitude 3 seconds after the initial P detection.

At large time, t , after the event origin time, the location estimates that maximize the posterior pdf (which are identical to those that maximize the likelihood function at large t) are robust amplitude-based locations can be used to verify arrival-based locations. In Figure 8, the amplitude-based location (green contours) is derived from the distribution of peak P- and S-wave amplitudes at 89 stations. The arrival-based location is obtained from 89 P-wave arrivals and an average P-wave velocity of 6 km/sec. The star marks the SCSN-reported location. There is general agreement between the amplitude- and arrival-based location estimates, indicating that the arrival-based location is most likely correct.

These estimates are independent of each other, as they are derived from different types of data.

3.2 16 October 1999 M7.1 Hector Mine, California earthquake: low station density

The M7.1 Hector Mine, California earthquake occurred in a region with relatively low density of SCSN stations. The closest station, HEC, was located 27 km north of the hypocenter. The mainshock, located by SCSN at 34.59N, 116.27W, at a depth of 5 km, was preceded by a cluster of 18 $1.5 \leq M \leq 3.8$ foreshocks within 1 km of the hypocenter in the previous 24 hours (Hauksson, 2002). The application of the VS method on the Hector Mine dataset illustrates the importance of prior information for regions with relatively low station density.

Figure 10 shows the operating SCSN stations (triangles), Voronoi cells (polygons), and seismicity in the preceding 24 hours (open circles) at the time of the mainshock. The areas of Voronoi cells of station HEC and adjacent stations range from 880 km^2 to 8020 km^2 ; these are an order of magnitude larger than the Voronoi cells in the epicentral region of the Yorba Linda earthquake.

The VS estimation process begins 3 seconds after the initial P detection at HEC, the first triggered station. Due to the large inter-station distances, the time between the initial P detection at station HEC and the P detection at the next closest station is 8 seconds. Figures 11(a) and 11(b) show the VS estimates at $\Delta t = 3$ and $\Delta t = 7$ seconds after the initial P detection at HEC. The regions of possible location consistent with HEC's Voronoi cell and the non-arrival information from the adjacent stations are shaded; these regions vary continuously as a function of time since the initial P detection. Within the regions of possible location, the most probable location estimates correspond to the locations where previously observed seismicity was concentrated. Thus, as early as 3 seconds after the initial P detection, with only one P arrival at the first triggered station, the VS location estimate agrees with the actual location (reported by SCSN). The 3-second magnitude estimate is $M = 6.2 \pm 0.45$; the 7-second magnitude estimate is $M = 7.2 \pm 0.45$.

Figure 12 shows the evolution of different magnitude estimates for the Hector Mine mainshock based on: 1) observed amplitudes only with no prior, 2) observed amplitudes with Voronoi cells, seismicity, and Gutenberg-Richter in the prior, and 3) similar to 2) but without the Gutenberg-Richter relationship. There are significant differences in these types of estimates in the early part of the estimation process, when observations are scarce; these different estimates converge and approach the SCSN-reported magnitude of M7.1 as more observations become available and the prior becomes less important with increasing t . When sufficient data is available, the estimates are driven by the observations (amplitudes and arrivals) and the choice of prior is irrelevant. The prior is important only in the early stages of the estimation process, where there is not sufficient data to adequately constrain the estimation process.

4. How subscribers might use early warning information

Ultimately, the goal of seismic early warning is to provide users with information that can be used to determine the optimal course of action in the few seconds before the onset of damaging ground motion levels at their sites of interest.

Consider the case of a subscriber who wants to initiate a predetermined set of damage-mitigating actions if the peak ground motions at the site of interest exceed a threshold level, $Y_{\max} > Y_{\text{thresh}}$. Given the early warning source estimates and their uncertainties, the expected ground motion levels can be predicted using attenuation relationships. The uncertainty on these predicted ground motion levels, σ_{pred} , is a combination of uncertainties from the early warning source estimates and uncertainties from the attenuation relationships. As additional observations become available, the uncertainties from the source estimates decrease; σ_{pred} approaches the uncertainty on the ground motion attenuation relationships. From Table 1, σ_{pred} for various amplitude types (horizontal and vertical acceleration, velocity, and displacement for P- and S-waves on rock and soil sites) is on the order of 0.3 log units, or a factor of 2. The probability of observing a maximum ground motion level Y_{\max} , given the predicted ground motions Y_{pred} from the early warning estimates, is

$$P(Y_{\max} | M, loc) = \frac{1}{\sqrt{2\pi}\sigma_{\text{pred}}} \exp\left[-\frac{(Y_{\max} - Y_{\text{pred}}(M, loc))^2}{2\sigma_{\text{pred}}^2}\right] \quad (12)$$

In Eqn.(12), Y_{pred} is the predicted maximum amplitude expected at the site of interest. These are given by the horizontal S-wave amplitude envelope attenuation relationships in Table 1. The probability of the ground motion threshold Y_{thresh} being exceeded, P_{ex} , given the early warning source estimates, is

$$P_{\text{ex}} = P(Y_{\max} > Y_{\text{thresh}} | Y_{\text{pred}}) = \int_{Y_{\text{thresh}}}^{\infty} P(Y_{\max} | M, loc) \quad (13)$$

At the time when the subscriber must decide whether to initiate actions or not, the actual peak ground motions at the site, Y_{\max} , are of course unknown; the decision to initiate actions or not must be based on some function of the predicted ground motions, Y_{pred} . The uncertainty in the relationship between Y_{\max} and Y_{pred} gives rise to the possibility of less than optimal decisions: 1) a false alarm corresponds to initiating action when it is ultimately unnecessary, or $Y_{\max} < Y_{\text{thresh}}$, and 2) a missed alarm corresponds to not initiating action when it is ultimately necessary, or $Y_{\max} > Y_{\text{thresh}}$.

The following is a simple cost-benefit analysis using basic decision theory for a subscriber who wants to initiate a set of actions if $Y_{\max} > Y_{\text{thresh}}$ (Grigoriou, 1979).

Let $H = h_i, i = 1, K, n$ be the (exhaustive and mutually exclusive) set of possible states of nature. In our example, $n = 2$; the only possibilities are 1) $Y_{\max} > Y_{\text{thresh}}$, or 2) $Y_{\max} < Y_{\text{thresh}}$. Let $B = b_j, j = 1, K, m$ be the set of possible actions. In our example, $m = 2$; the possible actions we consider are 1) “initiate actions”, and 2) “do nothing”. Let $C(b_j, h_i)$ be the cost of action b_j if the state of nature is h_i . Let P_i be the probability of h_i . C_{damage} is the cost of damage incurred if no actions were taken and the peak ground motions exceeded the threshold, $Y_{\max} > Y_{\text{thresh}}$; it is the cost of a missed alarm. C_{act} is the cost of performing the damage-mitigating actions; it is also the cost of a false alarm. For simplicity, assume that C_{damage} and C_{act} are known. In practice, these are also uncertain, and probability models are required to describe these quantities. The cost table, expressed in terms of $C_{\text{ratio}} = \frac{C_{\text{damage}}}{C_{\text{act}}}$ is shown in Table 2. The expected cost, $E[C_j]$, of a particular action is given by

$$E[C_j] = \sum_{i=1}^n C(b_j, h_i) P_i \quad (14)$$

The optimal action given a particular early warning source estimate is the action with the minimum cost. If we set $E[\text{"initiate action"}] = E[\text{"do nothing"}]$, we find the critical probability of exceedance, above which it is optimal to initiate action

$$P_{\text{ex,crit}} = \frac{1}{C_{\text{ratio}}} \quad (15)$$

Since $P_{\text{ex,crit}}$ is a probability, it takes on values between 0 and 1. This implies that $C_{\text{ratio}} \geq 1$; the cost of damage as a consequence of not acting must be equal to or greater than the cost of performing the actions, else early warning information provides no benefit to the subscriber.

We can relate $P_{\text{ex,crit}}$ to the predicted level of ground motion, $Y_{\text{pred,crit}}$, above which it is optimal to act

$$Y_{\text{pred,crit}} = Y_{\text{thresh}} - \sigma_{\text{pred}} \sqrt{2} \left[\text{erf}^{-1} \left(1 - \frac{\sqrt{2\pi} \sigma_{\text{pred}}}{C_{\text{ratio}}} \right) \right] \quad (16)$$

Thus, taking into account that there are uncertainties in the ground motion predictions from an early warning source estimate, the appropriate criteria for a subscriber to initiate action is $Y_{\text{pred}} > Y_{\text{pred,crit}}$ where $Y_{\text{pred,crit}}$ depends both on subscriber-specific values Y_{thresh} and C_{ratio} , as well as the uncertainty on the predicted ground motions σ_{pred} .

Figure 19 shows $Y_{\text{pred,crit}}$ as a function of σ_{pred} for various values of C_{ratio} . Y_{thresh} is simply a constant offset; in this plot, we set $Y_{\text{thresh}} = 0$. For subscribers with $C_{\text{ratio}} \sim 1$,

false alarms are relatively expensive; when σ_{pred} is large, it is sometimes optimal to “do nothing” even when the predicted ground motions exceed the threshold, $Y_{pred} > Y_{thresh}$. For subscribers with $C_{ratio} \gg 1$, false alarms are relatively inexpensive; it is optimal to initiate action even when $Y_{pred} < Y_{thresh}$. This highlights the importance of C_{ratio} in optimizing use of early warning information. Simple applications, such as opening fire station doors, or stopping elevators at the closest floor, would have relatively high values of C_{ratio} . Considerable application-specific efforts are required to determine what values of C_{ratio} would be appropriate for more complex applications such as diverting airport traffic, putting nuclear plants into safe mode, or stopping sensitive manufacturing equipment. Each subscriber needs to invest efforts into determining its appropriate C_{ratio} , and whether it is in fact a suitable candidate for early warning.

5. Station density and the evolution of estimate uncertainties

The uncertainties on early warning source estimates translate to uncertainties in predicted ground motions, which play an important role for users in decision-making using early warning information. In the VS method, the posterior density function is a three dimensional function in magnitude, latitude, and longitude. How should the network transmit the source estimates and their uncertainties to the subscribers? If the posterior density function can be described as a Gaussian, it may be sufficient to transmit 6 parameters (3 means, and 3 standard deviations) to the subscribers. The marginal probability density (integrating over latitude and longitude) of the magnitude estimate can always be described as a Gaussian, whether or not the Gutenberg-Richter law is included (Figure 13a, Figure 14a). This is not always the case for the latitude and longitude estimates. The simplest location estimate is to assume that the earthquake is located at the first triggered station. In regions with relatively high station density, this is a relatively good assumption to make. The maximum possible errors on such location estimates depend on inter-station distances. In regions where instrumentation density is high (for instance, the epicentral region of the Yorba Linda mainshock), this is a reasonable assumption, with maximum possible errors on the order of 10 km. In contrast, this assumption is inappropriate in regions with low station density or regions on the outer boundaries of the network. In the epicentral region of the Hector Mine earthquake, the maximum possible error in assuming the event is located at the first triggered station is 60 km (the maximum epicentral distance consistent with the Voronoi cell geometry). In less instrumented regions within SCSN, the maximum possible location error associated with such an assumption can be as large as 120 km. When station density is high, the posterior density function can be described by 3 Gaussian functions since 1) assuming a location at the first triggered station is appropriate, and 2) prior information is not necessary, since there are quickly enough arrivals to properly constrain the location.

When station density is low, assuming a location at the first triggered station can have very large errors. Prior information is important for the initial estimates in such regions, since large inter-station distances mean that it takes a while before there are enough observations to properly constrain the magnitude and location estimates. Prior information such as previously observed seismicity and known fault locations make the

latitude and longitude marginal density functions highly irregular and multimodal. It is prohibitive in terms of time and communications bandwidth for the network to transmit the full 3d posterior density function to subscribers. Nevertheless, it is necessary to provide this information to subscribers. An attractive alternative is for the network to transmit the likelihood function to the subscribers, and for the subscribers combine the prior and likelihood on site. This alternative provides the subscriber added flexibility in: 1) defining its own prior (for instance, whether or not to include the Gutenberg-Richter relationship), 2) determining computational resources (for instance, maximizing the posterior density function could be implemented on parallel processors).

It is particularly important for subscribers to have a control over whether or not the Gutenberg-Richter relationship should be included in the prior. Figure 16 shows the evolution of different magnitude estimates (amplitudes only, VS with Gutenberg-Richter in prior, VS without Gutenberg-Richter in prior) for 4 Southern California earthquakes. In all cases, the VS magnitude estimates converge to the magnitudes reported by SCSN once there are enough observations to properly constrain the estimates, regardless of the choice of prior. When there are trade-offs in the source parameters unresolved by the observed amplitudes, the VS magnitude estimates without the Gutenberg-Richter relationship have a smaller error compared to when the Gutenberg-Richter relationship is included. This seems to indicate that the information provided by the Gutenberg-Richter relationship is not useful. However, the Gutenberg-Richter relationship has been observed to hold in general worldwide. This apparent inconsistency is resolved by taking into account the user considerations. In these 4 cases, VS magnitude estimates with the Gutenberg-Richter relationship in the prior are smaller than the actual magnitude. Subscribers basing decisions on VS estimates with the Gutenberg-Richter relationship will lower their incidence of false alarms, at the cost of increasing their vulnerability to missed warnings. Thus, subscribers with $C_{ratio} \sim 1$ should consider using the Gutenberg-Richter relationship in their prior. In contrast, subscribers with $C_{ratio} \gg 1$ can exclude the Gutenberg-Richter relationship from their prior, and benefit from the smaller errors in the magnitude estimates. Such subscribers have relatively high costs for missed warnings. Since they place a premium on making the appropriate decisions during the large, infrequent events, they need to accept a certain level of false alarms dictated by C_{ratio} . More studies regarding how VS estimates evolve with time are necessary.

6. Conclusions

The Virtual Seismologist (VS) method is a Bayesian approach that provides a unified framework for addressing both the real-time source estimation and the user-response problems in earthquake early warning. Disparate types of information, such as previously observed seismicity, station locations, and the Gutenberg-Richter relationship, are included in the source estimation problem via the Bayes prior. The trade-offs in the initial source estimates that cannot be resolved by the available data are resolved in favor of the prior information. The evolution of source estimates as a function of available data is similar to how humans modify their opinions or judgments in light of new information; prior information is important when data is sparse, but decreases in influence as additional observations become available.

What type of information to include in the Bayes prior, and hence, what type of source estimates to solve for, is dependent on user-specific considerations, in particular, the relative cost of missed to false alarms. Users with relatively expensive false alarms should include the Gutenberg-Richter relationship in the prior, at the cost of increasing their vulnerability to missed warnings. Users with relatively expensive missed alarms should use source estimates excluding the Gutenberg-Richter relationship. A certain level of false alarms must be accepted if the aim is to act appropriately during the large, infrequent earthquakes.

7. Acknowledgements

We wish to thank Hiroo Kanamori, Egill Hauksson, James Beck, and John Clinton for their stimulating discussions and for their comments on the thesis work on which this manuscript is based. This work was supported by the Department of Civil Engineering at the California Institute of Technology. The completion of the manuscript was made possible with support of the Puerto Rico Seismic Network and the Puerto Rico Strong Motion Program.

8. References

- Allen, R. M. and H. Kanamori (2003). The potential for earthquake early warning in Southern California. *Science* **300**, 786-789.
- Cua, G. (2005). Creating the Virtual Seismologist: developments in ground motion characterization and seismic early warning. PhD thesis, California Institute of Technology. <http://resolver.caltech.edu/CaltechETD:etd-02092005-125601>.
- Cua, G. and T. Heaton (2006). Characterizing average properties of Southern California ground motion envelopes. (*in preparation*)
- Cua, G. and T. Heaton (2006). Linear discriminant analysis in earthquake early warning. (*in preparation*)
- Gerstenberger, M., S. Wiemer, and L. Jones (2003). Real-time forecasts of tomorrow's earthquakes in California: a new mapping tool. *United States Geological Survey Open File Report, 2004-1390*.
- Goltz, J. D. (2002). Introducing earthquake early warning in California: a summary of social science and public policy issues. *Technical Report, Governor's Office of Emergency Services*.
- Grazier, V., A. Shakal, C. Scrivner, E. Hauksson, J. Polet, and L. Jones (2002). TriNet strong-motion data from the M7.1 Hector Mine, California earthquake of 16 October 1999. *Bull. Seism. Soc. Am.* **92**, 1525-1542.
- Grigoriu, M., D. Veneziano, and C. A. Cornell (1979). Probabilistic modeling as decision making. *Journal of the Engineering Mechanics Division, ASCE EM4*, 585-596.
- Hauksson, E., K. Hutton, L. Jones, and D. Given (2002). The September 03, 2002 earthquake M4.6 near Yorba Linda. <http://www.trinet.org/eqreports>
- Hauksson, E., L. Jones, and K. Hutton (2002). The 1999 M_w7.1 Hector Mine, California earthquake sequence: complex conjugate strike-slip faulting. *Bull. Seism. Soc. Am.* **92**, 1154-1170.
- Heaton, T. (1985). A model for a seismic computerized alert network. *Science* **228**, 987-990.
- Horiuchi, S., H. Negishi, K. Abe, A. Kimimura, and Y. Fujinawa. An automatic processing system for broadcasting earthquake alarms. *Bull. Seism. Soc. Am.* **95**, 708-718.
- Jones, L. (1984). Foreshocks (1966-1980) in the San Andreas system, California. *Bull. Seism. Soc. Am.* **74**, 1361-1380.

- Kanamori, H. (1993). Locating earthquakes with amplitude: application to real-time seismology. *Bull. Seism. Soc. Am.* **83**, 264-268.
- Nakamura, Y. (1988). On the urgent earthquake detection and alarm system (UrEDAS). *Proceedings of 9th World Conference in Earthquake Engineering*, Tokyo-Kyoto, Japan.
- Rydelek, P. and J. Pujol (2004). Real-time seismic warning with a 2-station subarray. *Bull. Seism. Soc. Am.* **94**, 1546-1550.
- Sivia, D.S. (1996). *Data Analysis: a Bayesian tutorial*. Oxford University Press.
- Wu, Y.M. and H. Kanamori (2005a). Experiment on an onsite early warning method for the Taiwan early warning system. *Bull. Seism. Soc. Am.* **95**, 347-353.
- Wu, Y.M. and H. Kanamori (2005b). Rapid assessment of damaging potential of earthquakes in Taiwan from the beginning of P waves, *Bull. Seism. Soc. Am.* **95**, 1181-1185.
- Yamada, M. and T. Heaton (2006). Early warning systems for large earthquakes: estimation from fault location using ground motion envelopes, *Bull. Seism. Soc. Am.* (submitted)

9. Figure captions

Figure 1: Magnitude plotted against ground motion ratio

$$Z_{obs} = 0.36 \log(PVA) - 0.93 \log(PVD) \text{ for P-wave amplitudes.}$$

Figure 2: Prior information for Yorba Linda, California earthquake: SCSN station locations (triangles), associated Voronoi cells (polygons), and seismicity in the preceding 24 hours (open circles) within 200 km of the mainshock (star). Two foreshocks occurred within the Voronoi cell of station SRN (shaded), the station closest to the epicenter.

Figure 3: Range of possible Yorba Linda earthquake epicentral distances from station SRN consistent with a first P detection at SRN (scaled such that maximum on y axis is 1). The weights on various distances (y axis) are obtained by giving equal weight to all locations within SRN's Voronoi cell. The most probable epicentral distance (8 km) is that which occurs most often within SRN's Voronoi cell. If we had included seismicity information in the prior, that there were two foreshocks at the mainshock epicenter means this distribution would include an impulse function situated at the distance of the mainshock.

Figure 4: Contours of the likelihood function for the $M = 4.75$ Yorba Linda earthquake expressed in terms of magnitude and epicentral distance using the peak amplitudes at SRN 3 seconds after the initial P detection (no prior information, only the peak amplitudes observed at SRN). The peak of the likelihood function is scaled to 1, and contours are drawn at 0.6, 0.1, and 0.01 levels. Regions where the likelihood function has a scaled value exceeding 0.6 are shaded. The likelihood function has a maximum at $M = 5.5$, $R = 33$ km. Elongated regions of equal probability indicate trade-offs in M , R unresolved by the available amplitudes and the attenuation relationships. The ground motion ratio term of the likelihood function constraints the possible magnitude to the approximate range $5 < M < 6$. The star marks the actual magnitude and epicentral distance to SRN of the Yorba Linda mainshock, $M = 4.75$, $R = 9.8$ km.

Figure 5: Contours of the posterior density function showing the effect of including the Gutenberg-Richter magnitude-frequency relationship in the prior on initial M , R estimates 3 seconds after the initial P detection. Figures 4a and 4b include the constraint on epicentral distance from the Voronoi cell of station SRN. Figure 4a includes the Gutenberg-Richter relationship as a constraint on magnitude, while Figure 4.b does not. The star marks the actual magnitude and epicentral distance of the Yorba Linda mainshock. The cross marks the VS estimates in $M.R$ space. The Gutenberg-Richter relationship favors smaller magnitude events located at smaller epicentral distances from the station. While inclusion of the Gutenberg-Richter relationship (a) produces magnitude estimates that are systematically smaller than the actual magnitudes, Bayesian statistics assure us that this is the most probable solution.

Figure 6: Snapshots of the likelihood function expressed as a function of magnitude and epicentral location at various magnitude ranges. The shaded regions in each subplot are locations consistent with the peak amplitudes available at station SRN 3 seconds after the

initial P detection. The trade-offs in magnitude and location are similar to those shown in Figure 3. If no prior information regarding station geometries, previously observed seismicity, or the Gutenberg-Richter relationship is included, we cannot distinguish between a small event at small epicentral distance from a large event at large distance.

Figure 7: VS estimates 3 seconds after the initial P detection at SRN for the Yorba Linda earthquake. Colors scale with probability that the event is located at the given location. The VS location estimate (indicated by an arrow) is within 2 km of the SCSN reported location. Prior information includes previously observed seismicity (open circles), Voronoi cell information, and available arrivals at adjacent stations. Contours show the VS magnitude estimates at a given location without the Gutenberg-Richter relationship in the prior. The VS magnitude estimate without the Gutenberg-Richter relationship ($M = 4.8 \pm 0.425$) is in good agreement with the SCSN-reported magnitude of $M = 4.75$.

Figure 8: Comparison of amplitude- and arrival-based location estimates 80 seconds after the origin time of the Yorba Linda earthquake. The amplitude-based location (green contours) is derived from the distribution of peak P- and S-wave amplitudes at 89 stations. The arrival-based location is obtained from 89 P-wave arrivals and an average P-wave velocity of 6 km/sec. The star marks the SCSN-reported location. There is general agreement between the amplitude- and arrival-based location estimates. These estimates are independent of each other, as they are derived from independent datasets.

Figure 9: The evolution of various magnitude estimates for the Yorba Linda earthquake as a function the duration of data from the seismic network. Estimates labeled “amplitudes only” correspond to magnitude estimates obtained by maximizing the likelihood function (no prior information). We distinguish between 2 VS magnitude estimates (both with station geometry and previously observed seismicity included in the prior) with and without the Gutenberg-Richter magnitude-frequency relationship in the Bayes’ prior. All magnitude estimates converge to the SCSN solution at large times, when there are sufficient available observations. The differences in the magnitude estimates in the earlier estimates are due to the differences in prior information included. The VS estimate without the Gutenberg-Richter relationship is within 0.05 magnitude units of the SCSN-reported magnitude 3 seconds after the initial P detection.

Figure 10: Operational SCSN stations (triangles), associated Voronoi cells (polygons), and seismicity in the preceding 24 hours (open circles) within 200 km of the $M=7.1$ Hector Mine, California mainshock (star). Eighteen earthquakes occurred within 1-km epicentral distance of the mainshock hypocenter.

Figure 11: VS estimates 3 and 7 seconds after the initial P detection at HEC for the Hector Mine earthquake. Colors scale with the probability that the earthquake is located at a given location. The shaded regions are the regions of likely location consistent with the initial P arrival at HEC, and no subsequent arrivals at adjacent stations 3 and 7 seconds later. Within the regions of likely location, the most probable locations are where there was a concentration of seismic activity in the preceding 24 hours. With Voronoi

cells and not-yet-arrived data, the VS location estimates continually evolve, even before the second P arrival. The likelihood function is based on peak amplitudes available at HEC 3 seconds after the initial P detection. Contours show the VS magnitude estimates at a given location without the Gutenberg-Richter relationship in the prior.

Figure 12: The evolution of various magnitude estimates for the Hector Mine earthquake as a function of duration of data from the network. The estimates labeled “amplitude only” correspond to the magnitudes that maximize the likelihood function (that is, no prior information included). VS magnitude estimates with and without the Gutenberg-Richter relationship in the Bayes prior are also shown.

Figure 13: In regions with high station density, such as the epicentral region of the Yorba Linda earthquake, assuming that the earthquake is located at the first triggered station is a valid assumption. The marginal pdfs for the VS magnitude and location estimates can be approximated as Gaussian distributions. The relevant information about the early warning estimates can be summarized by 6 parameters (3 means, and 3 standard deviations), which can be easily transmitted to subscribers.

Figure 14: In regions with low station density, such as the epicentral region of the Hector Mine earthquake, the initial VS estimates are heavily influenced by prior information. While the marginal pdf for the magnitude estimate can still be expressed as a Gaussian distribution, the marginal pdfs for the location estimates are non-Gaussian, due to the influence of previously observed seismicity.

Figure 15: The critical predicted level of ground motion above which early warning subscribers should initiate action, $Y_{pred,crit}$, as a function of uncertainty on predicted ground motions σ_{pred} and C_{ratio} . Depending on the value of C_{ratio} , it may be cost-effective for an early warning subscriber to initiate action even when the predicted ground motion levels are below the threshold at which damage occurs, Y_{thresh} .

Figure 16: The evolution of different magnitude estimates (amplitudes only, amplitudes with prior including Gutenberg-Richter relationship, and amplitudes with prior excluding the Gutenberg-Richter relationship) as a function of duration of data from the network for selected Southern California earthquake datasets. Estimates with the Gutenberg-Richter relationship in the prior reduce the probability of false alarms. Subscribers should have the flexibility to decide which type of magnitude estimates are best suited to their applications, based on their relative cost of missed to false alarms.

10. Tables and Figures

Table 1: Attenuation relationships for peak P- and S-wave amplitudes

$\bar{Y}(M, R) = aM + b(R_1 + C(M)) + d(R_1 + C(M)) + e + \alpha$ $R_1 = \sqrt{R + 9}$ $C(M) = c_1 \left(\arctan(M - 5) + \frac{\pi}{2} \right) \times \exp(c_2(M - 5))$										
				a	b	c ₁	c ₂	d	e	σ
Root mean square horizontal amplitudes	P-wave	Acceleration	rock	0.72	3.3x10 ⁻³	1.6	1.05	1.2	-1.06	0.31
			soil	0.74	3.3x10 ⁻³	2.41	0.95	1.26	-1.05	0.29
		velocity	rock	0.80	8.4x10 ⁻⁴	0.76	1.03	1.24	-3.103	0.27
			soil	0.84	5.4x10 ⁻⁴	1.21	0.97	1.28	-3.13	0.26
		displacement	rock	0.95	1.7x10 ⁻⁷	2.16	1.08	1.27	-4.96	0.28
			soil	0.94	-5.17x10 ⁻⁷	2.26	1.02	1.16	-5.01	0.3
	S-wave	acceleration	rock	0.78	2.6x10 ⁻³	1.48	1.11	1.35	-0.64	0.31
			soil	0.84	2.3x10 ⁻³	2.42	1.05	1.56	-0.34	0.31
		velocity	rock	0.89	4.3x10 ⁻⁴	1.11	1.11	1.44	-2.60	0.28
			soil	0.96	8.3x10 ⁻⁴	1.98	1.06	1.59	-2.35	0.30
		displacement	rock	1.03	1.01x10 ⁻⁷	1.09	1.13	1.43	-4.34	0.27
			soil	1.08	1.2x10 ⁻⁶	1.95	1.09	1.56	-4.1	0.32
Vertical amplitudes	P-wave	acceleration	rock	0.74	4.01x10 ⁻³	1.75	1.09	1.2	-0.96	0.29
			soil	0.74	5.17x10 ⁻⁷	2.03	0.97	1.2	-0.77	0.31
		velocity	rock	0.82	8.54x10 ⁻⁴	1.14	1.11	1.36	-0.21	0.26
			soil	0.81	2.65x10 ⁻⁶	1.4	1.0	1.48	-2.55	0.30
		displacement	rock	0.96	1.98x10 ⁻⁶	1.66	1.16	1.34	-4.79	0.28
			soil	0.93	1.09x10 ⁻⁷	1.5	1.04	1.23	-4.74	0.31
	S-wave	acceleration	rock	0.78	2.7x10 ⁻³	1.76	1.11	1.38	-0.75	0.30
			soil	0.75	2.47x10 ⁻³	1.59	1.01	1.47	-0.36	0.30
		velocity	rock	0.90	1.03x10 ⁻³	1.39	1.09	1.51	-2.78	0.25
			soil	0.88	5.41x10 ⁻⁴	1.53	1.04	1.48	-2.54	0.27
		displacement	rock	1.04	1.12x10 ⁻⁵	1.38	1.18	1.37	-4.74	0.25
			soil	1.03	4.92x10 ⁻⁶	1.55	1.08	1.36	-4.57	0.28

Table 2: Cost table for early warning subscriber

h_i	$P_i = P(h_i Y_{pred})$	“Do nothing”	“Initiate actions”
$Y > Y_{thresh}$	P_{ex}	C_{ratio}	1
$Y < Y_{thresh}$	$1 - P_{ex}$	0	1

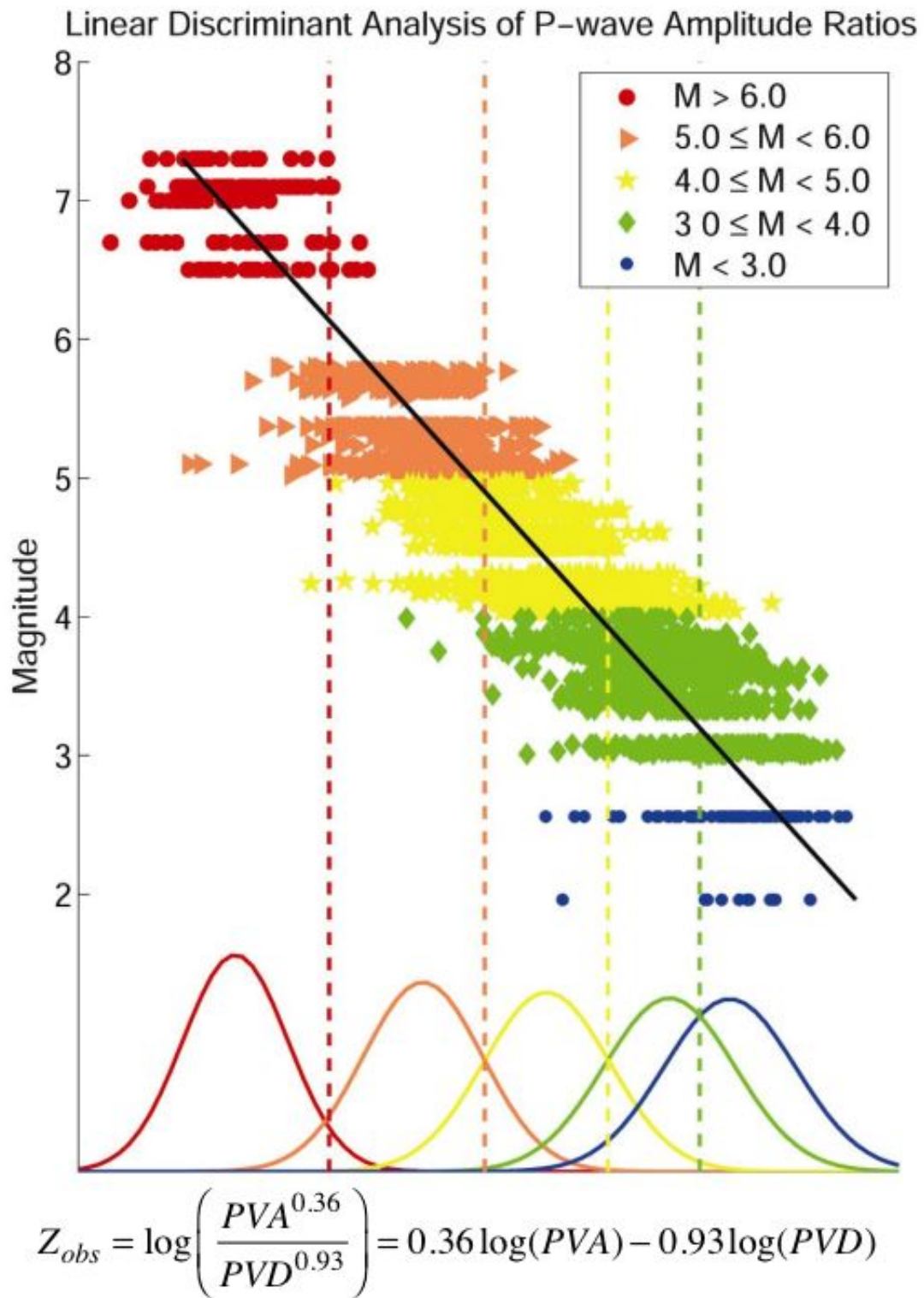


Figure 1

3 Sept 2002 M=4.75 Yorba Linda, California earthquake

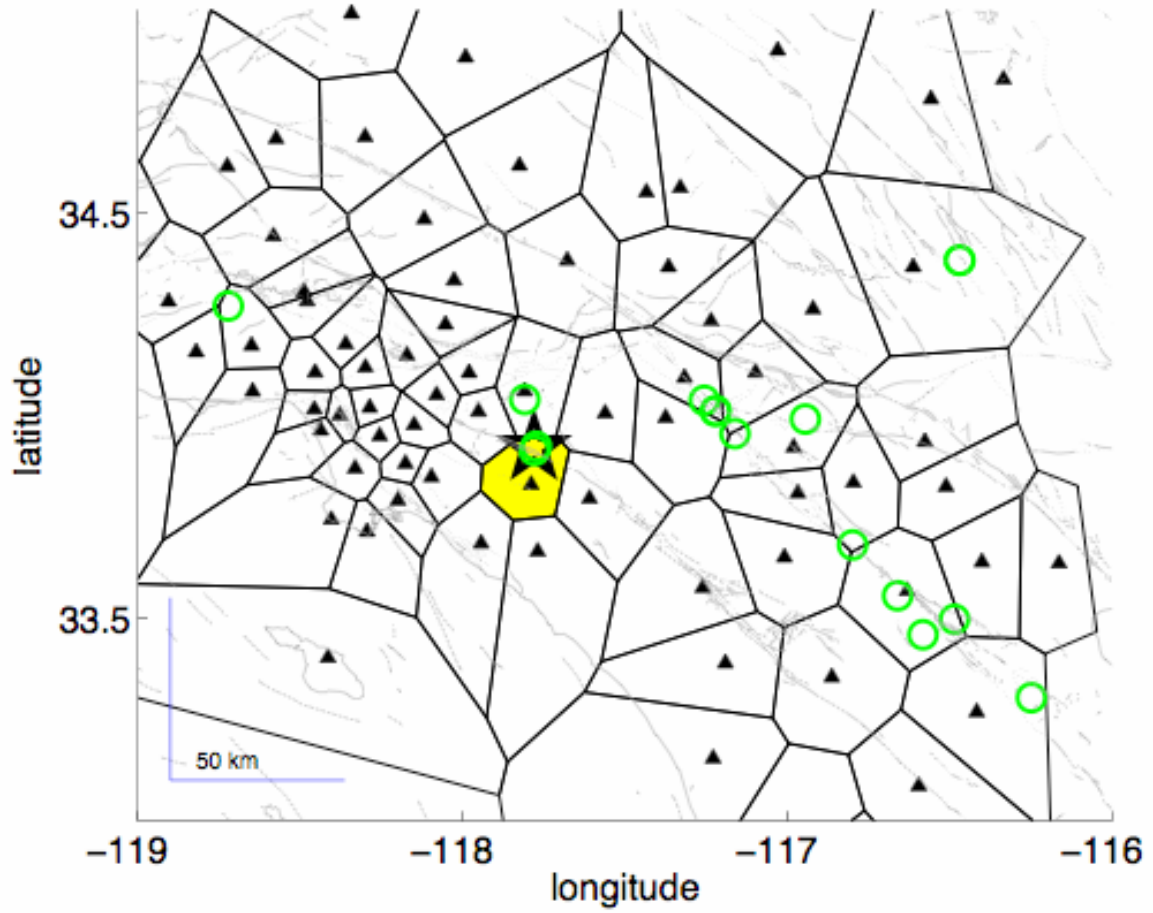


Figure 2

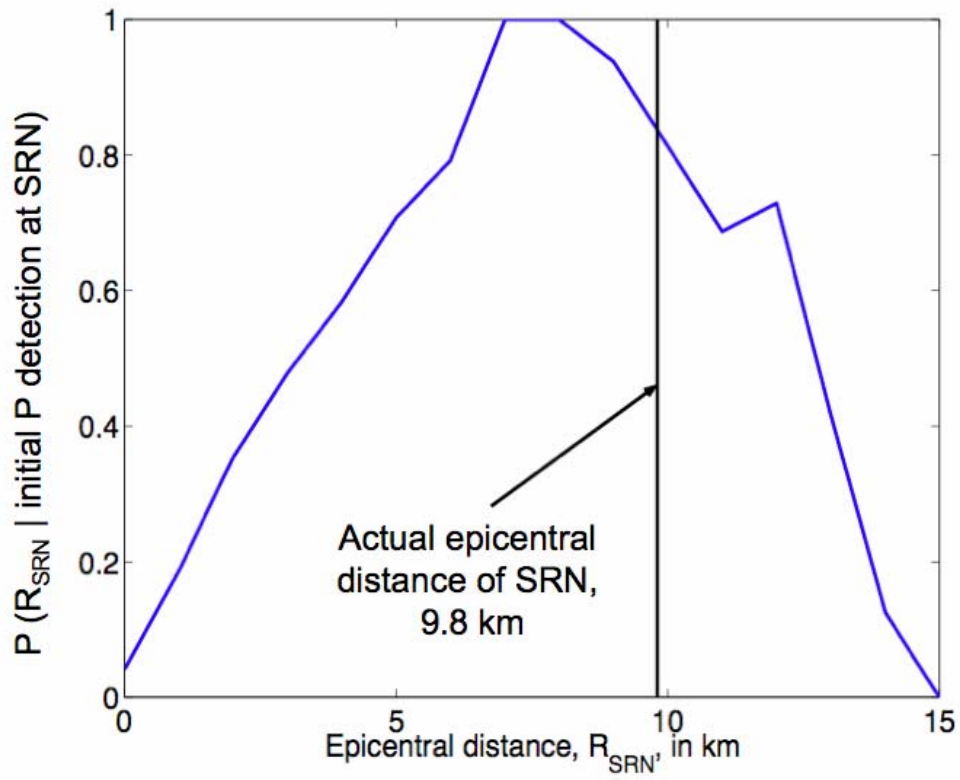


Figure 3

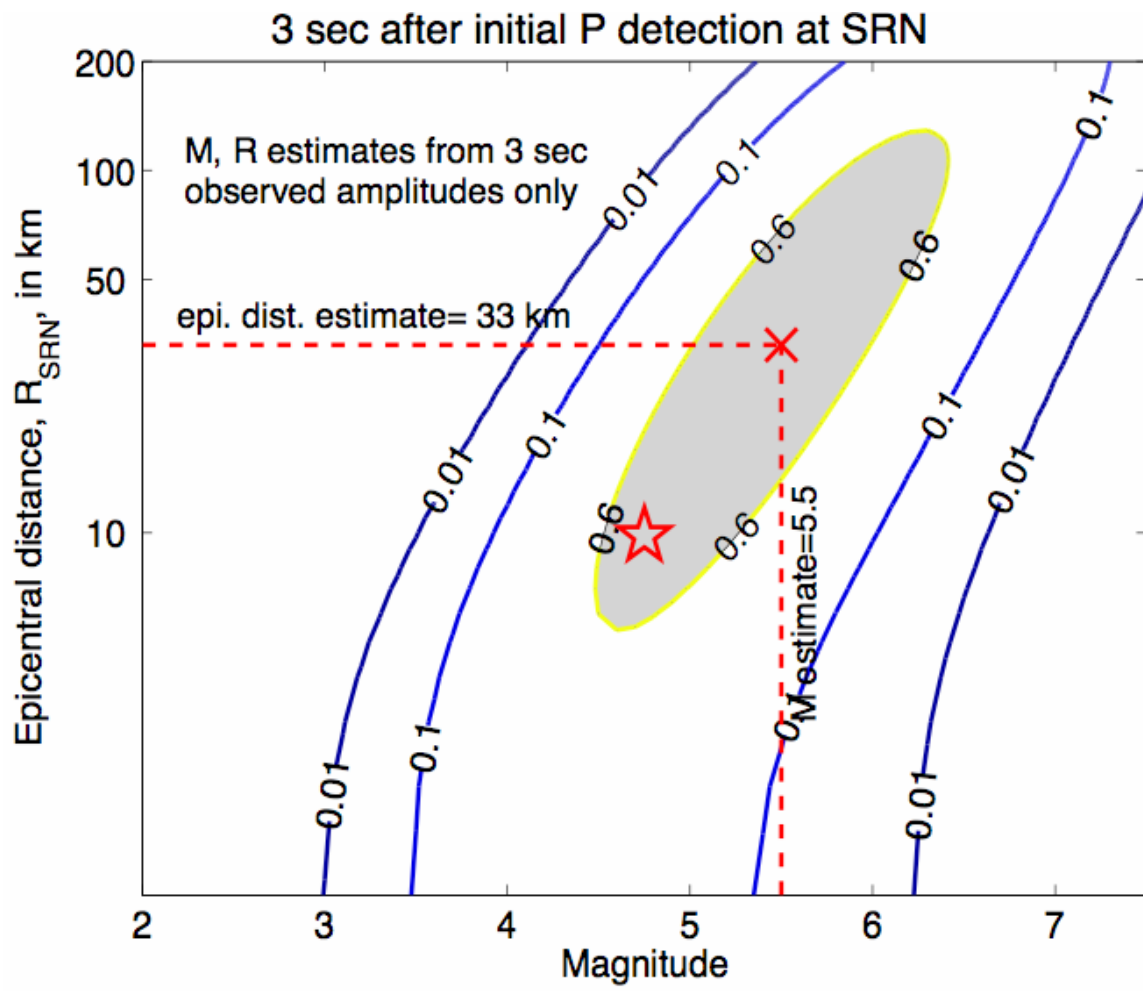


Figure 4

VS M, R estimates 3 sec after initial P detection at SRN

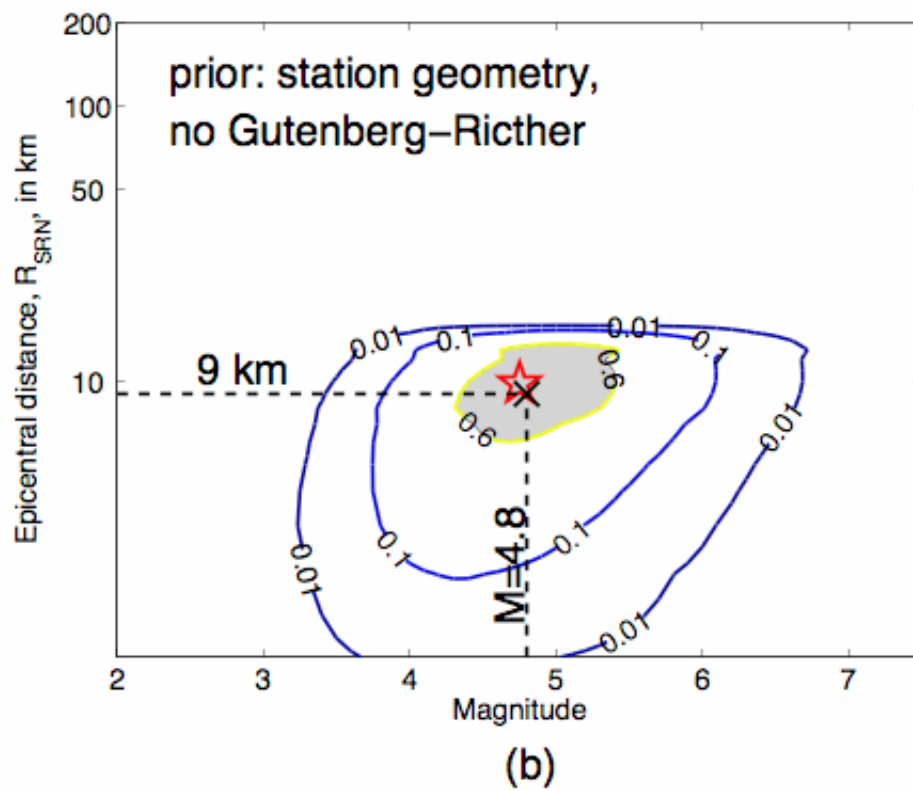
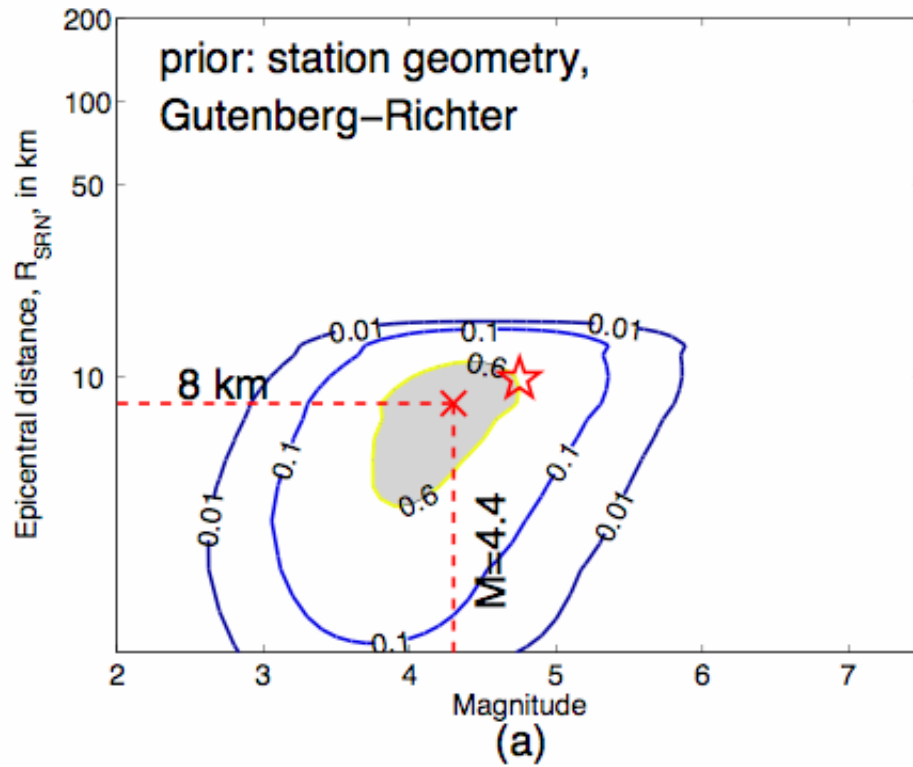


Figure 5

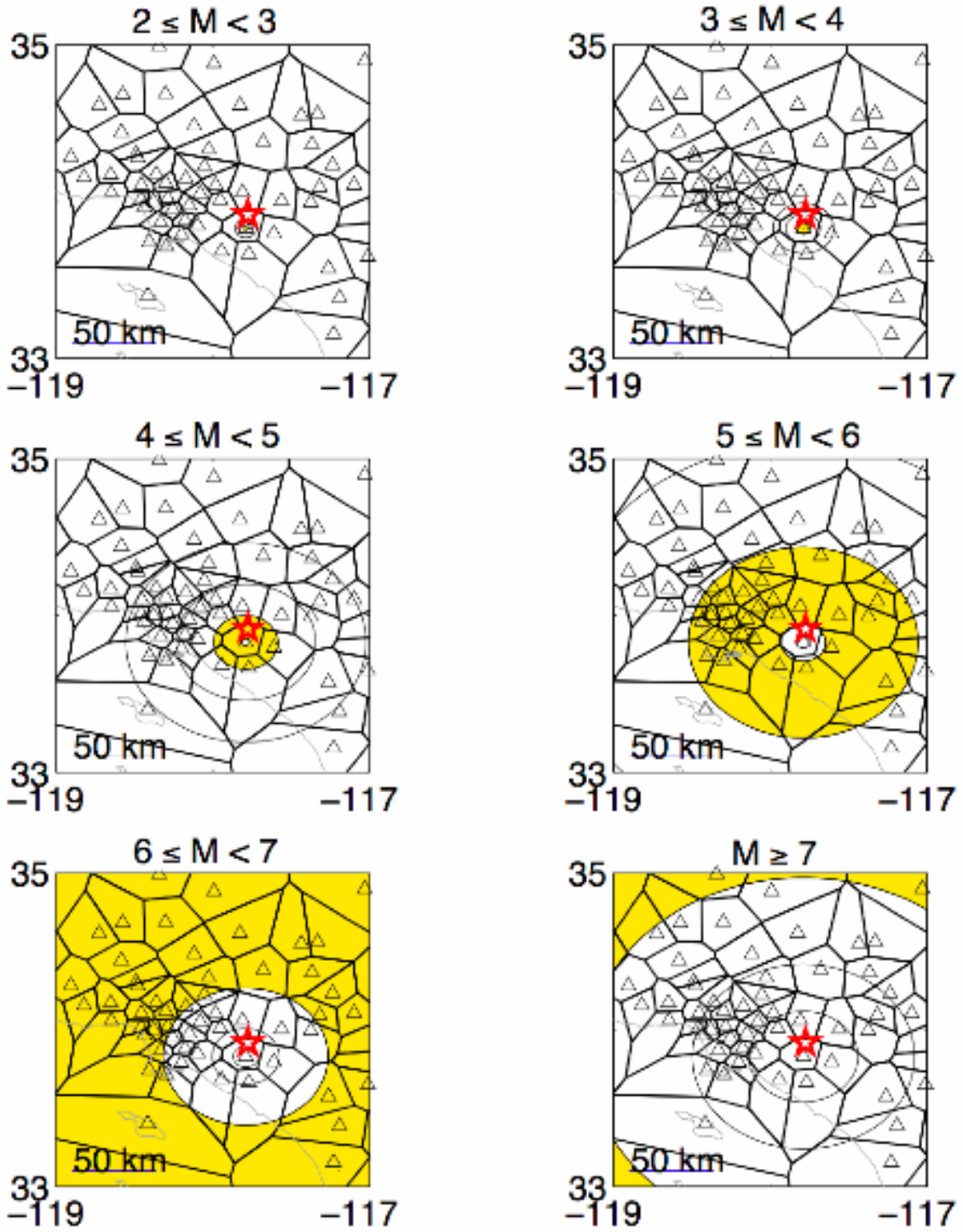


Figure 6

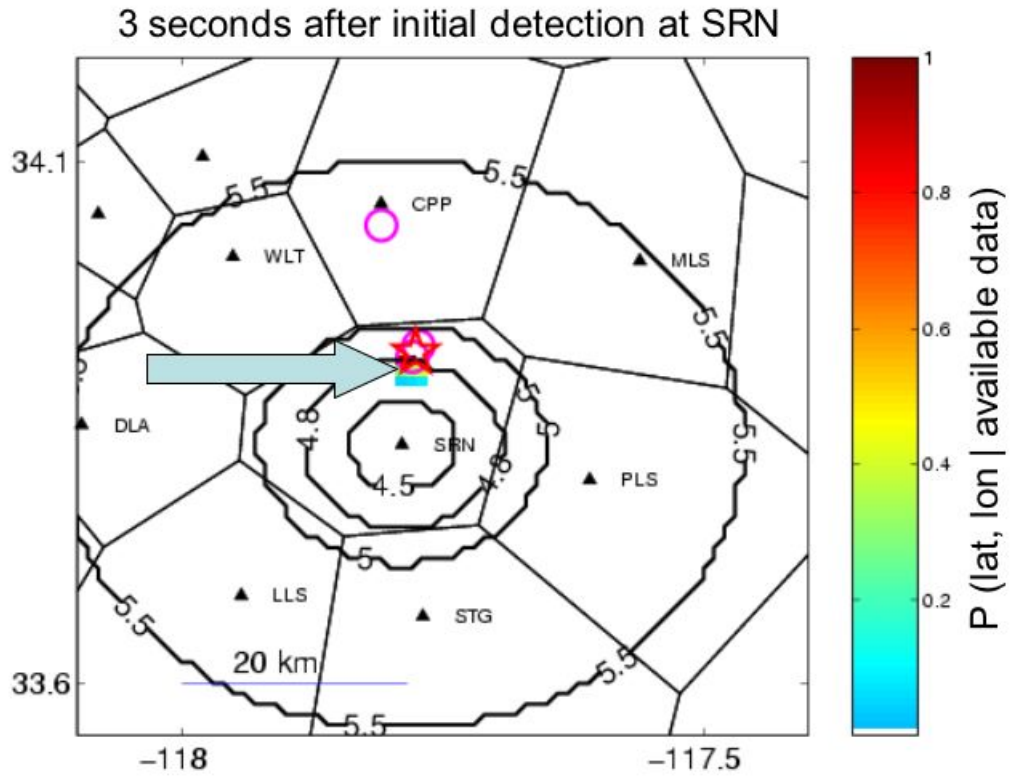


Figure 7

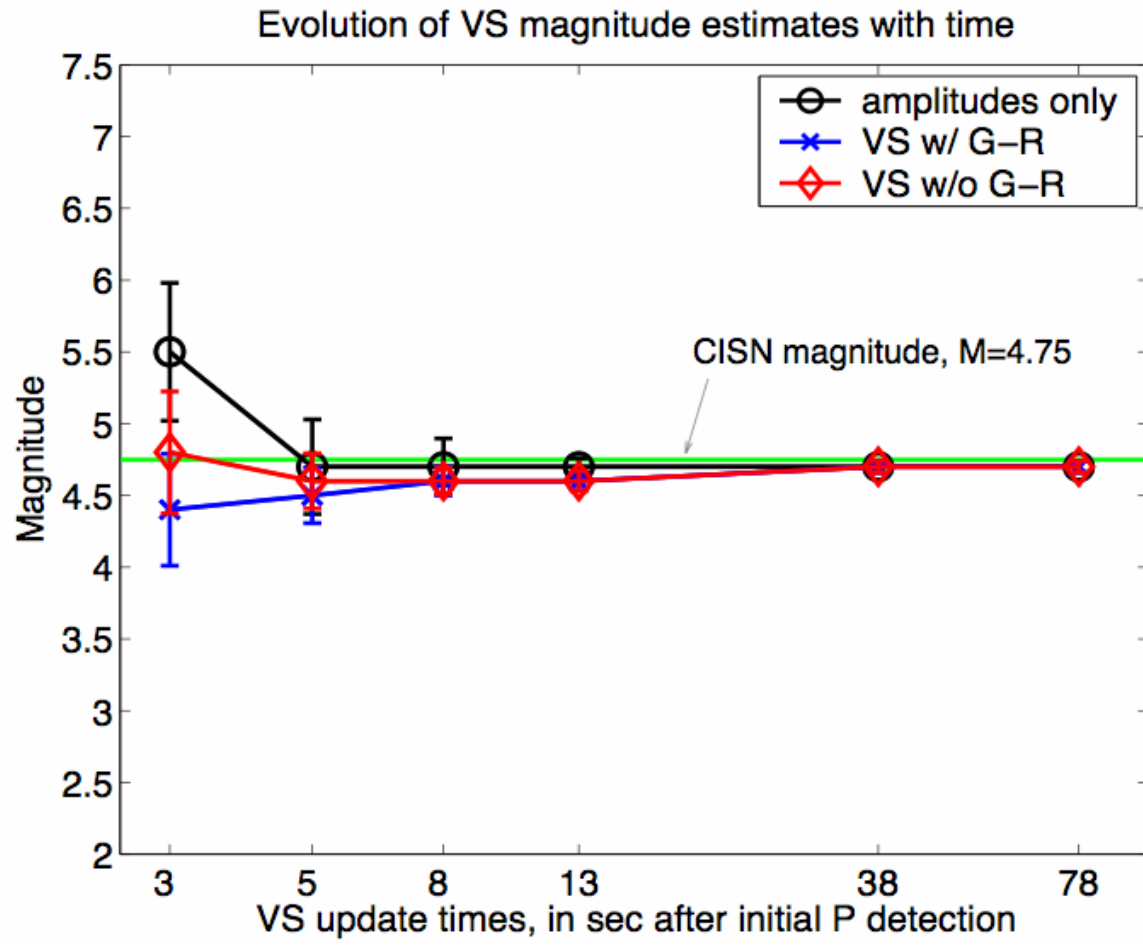


Figure 8

78 sec after initial P detection at SRN

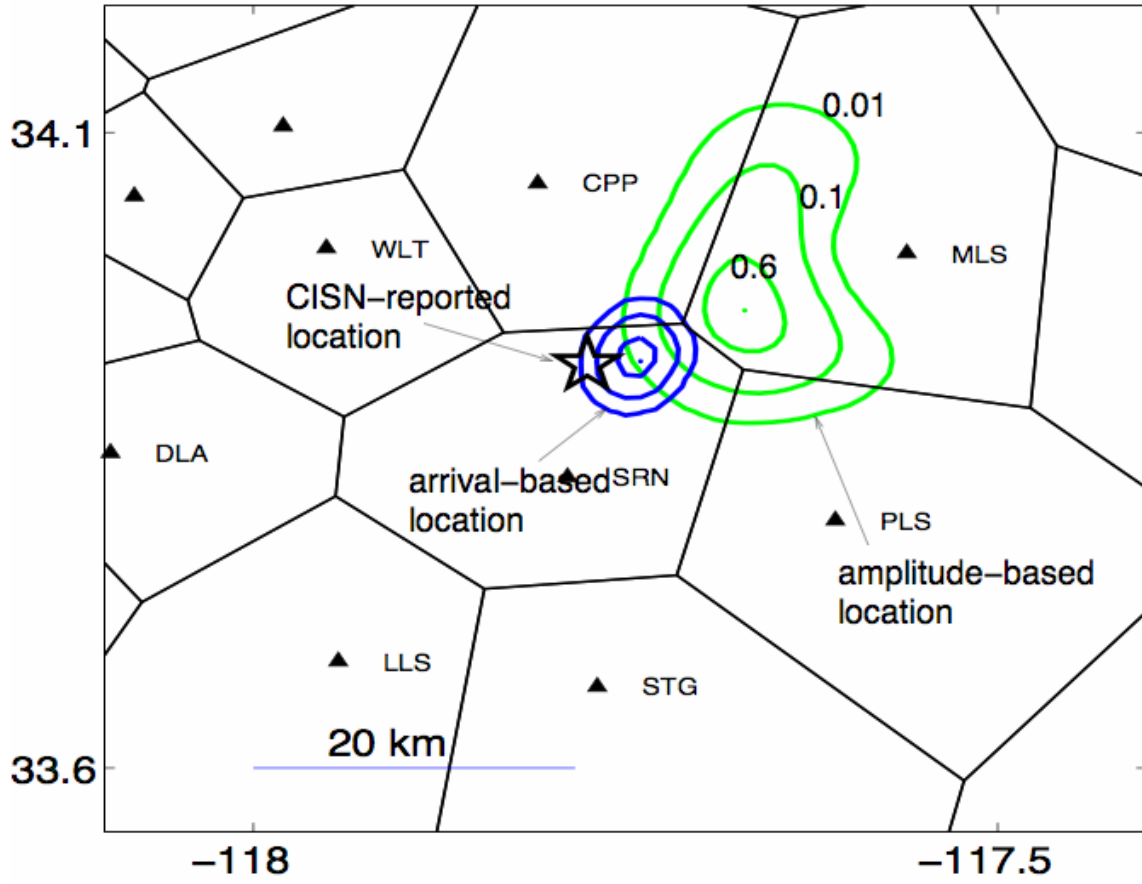


Figure 9

16 October 1999 M=7.1 Hector Mine, California earthquake

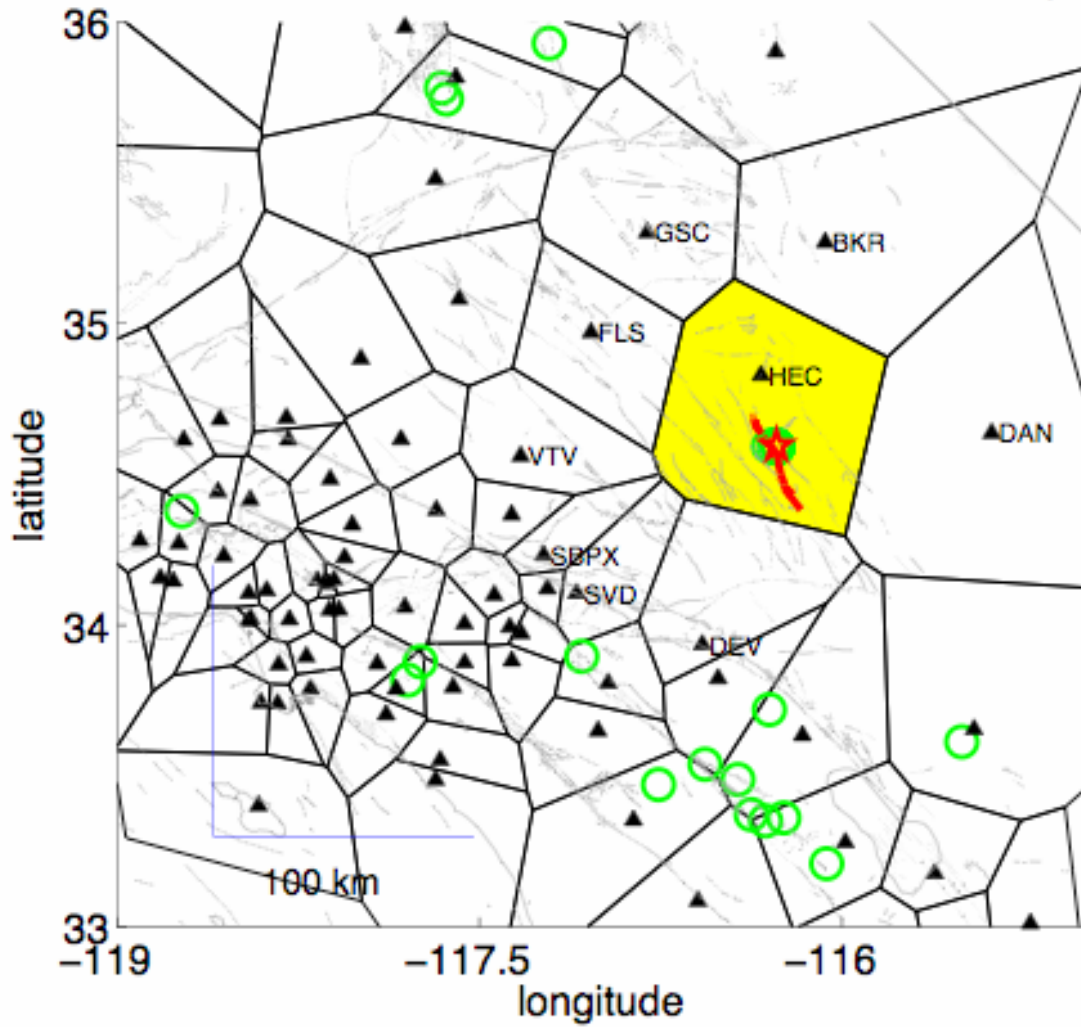
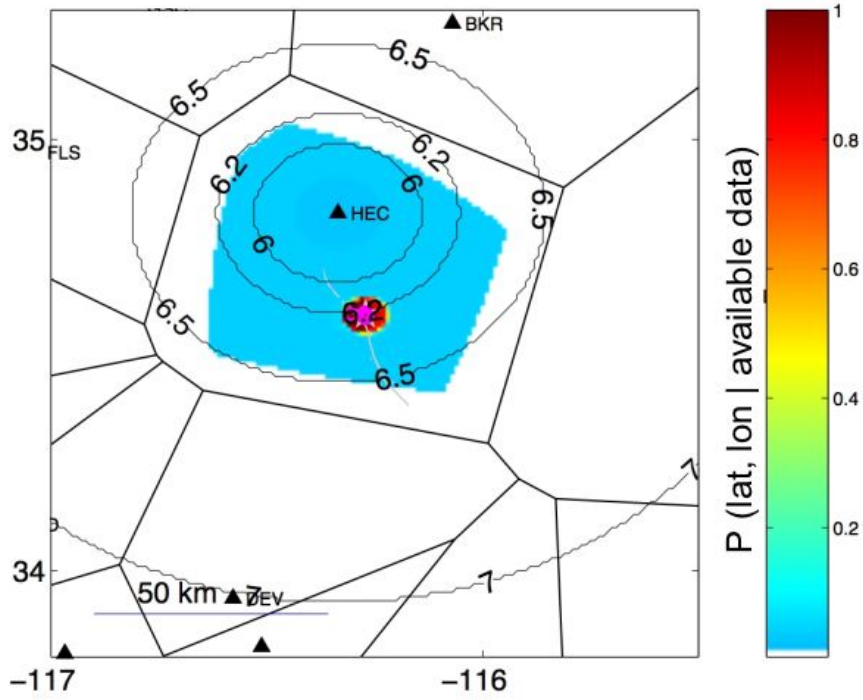


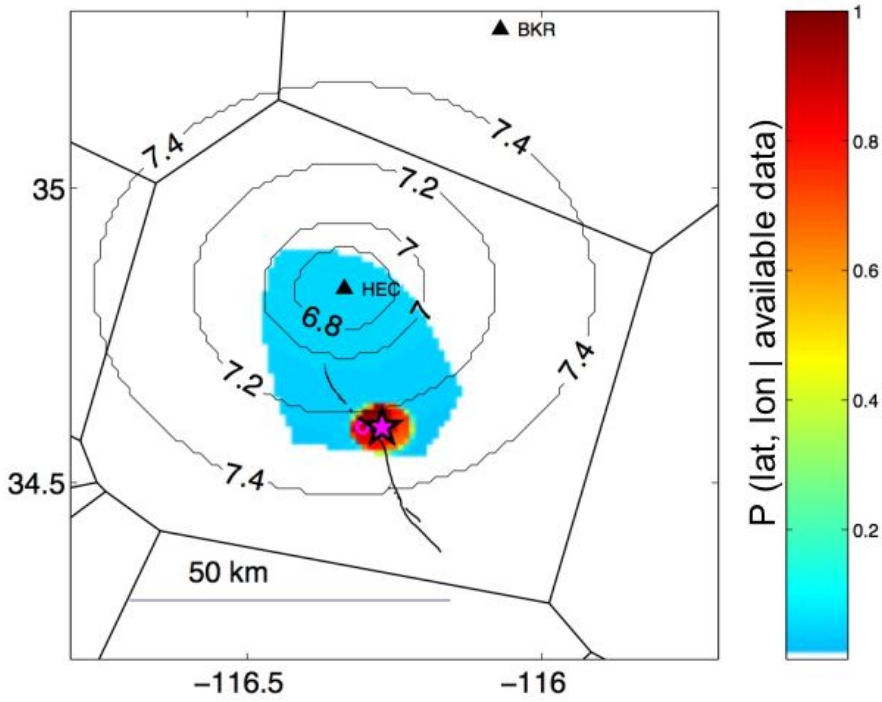
Figure 10

3 sec after initial P detection at HEC (1 station, no GR)



(a)

7 sec after initial P at HEC (no GR)



(b)

Figure 11

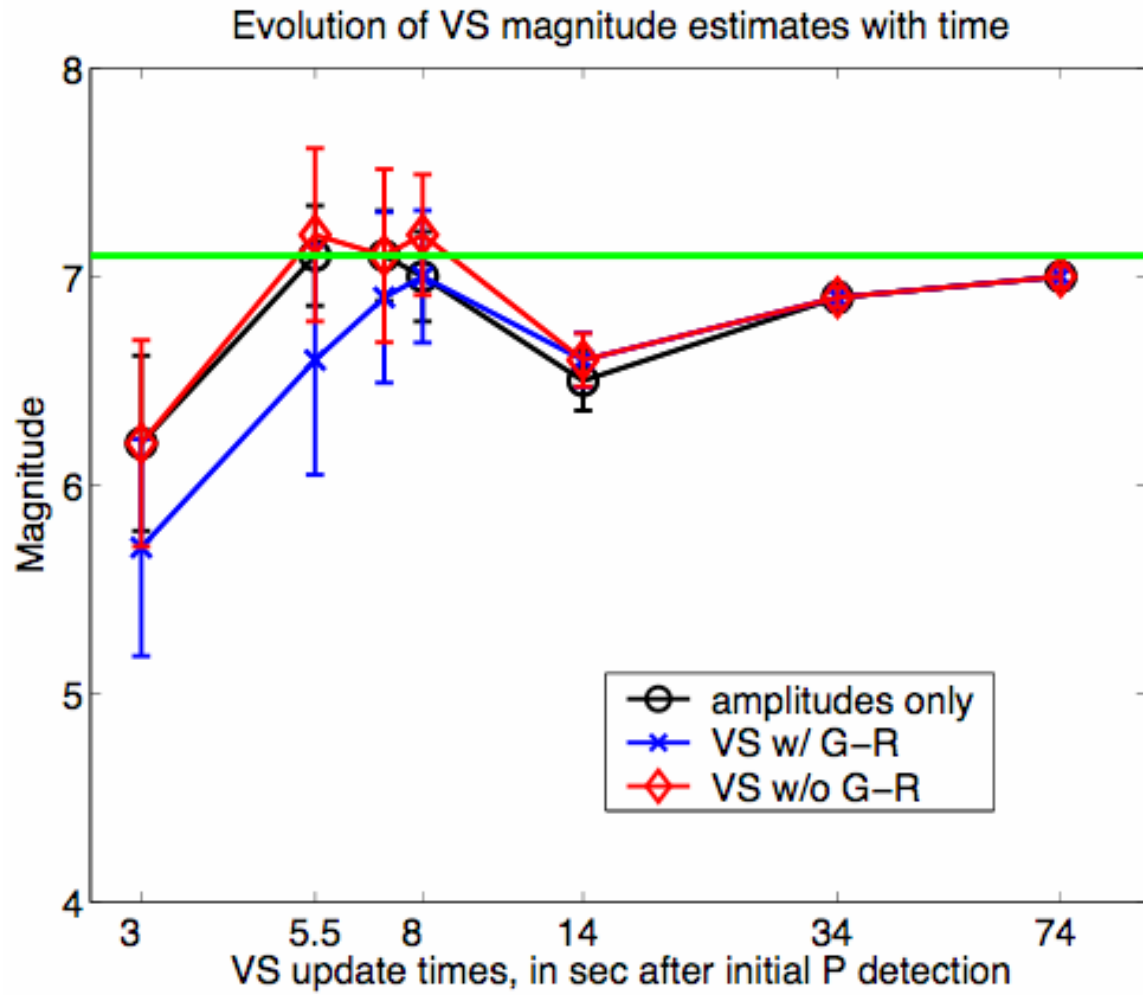


Figure 12

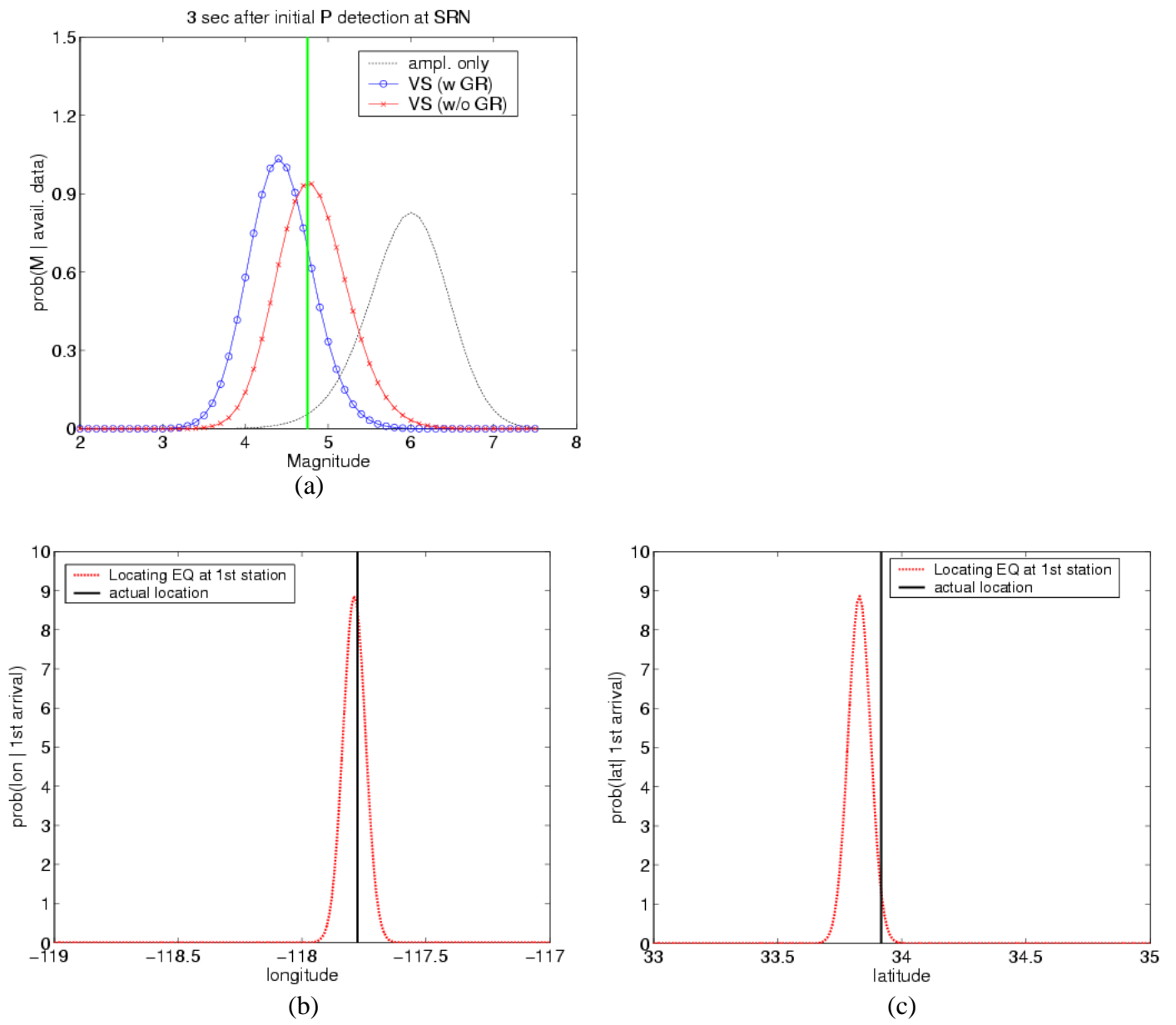
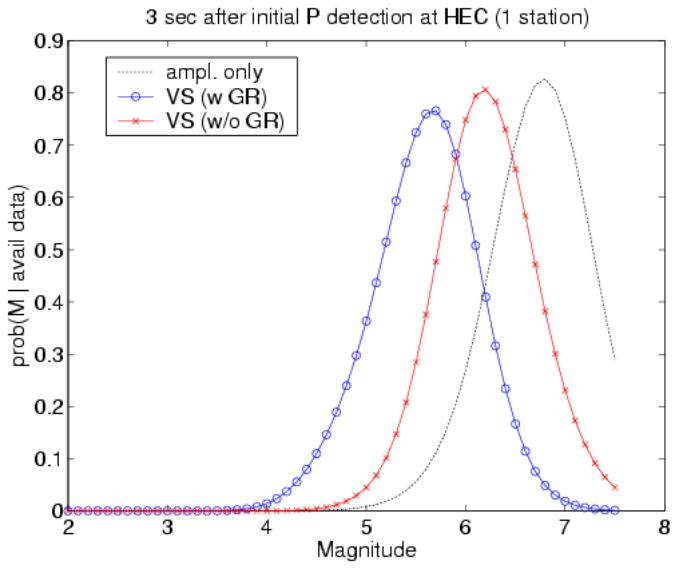
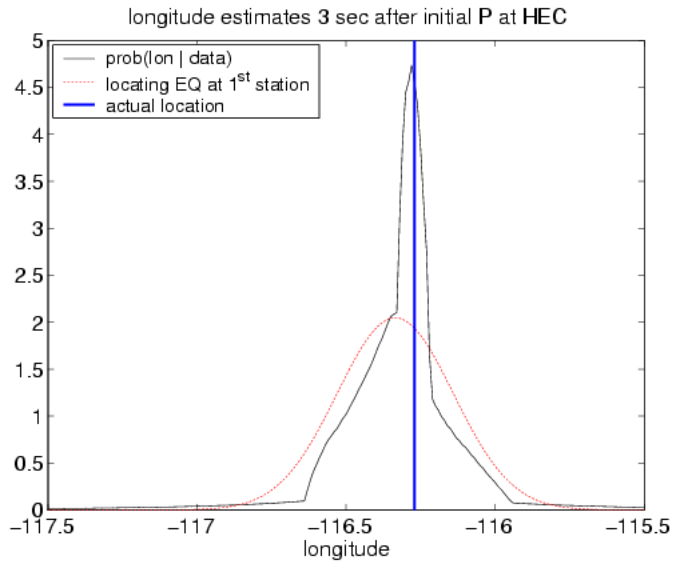


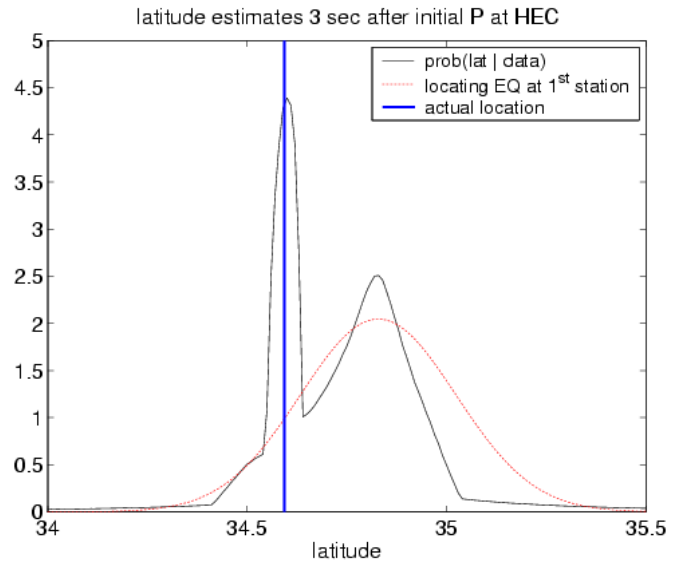
Figure 13



(a)



(b)



(c)

Figure 14

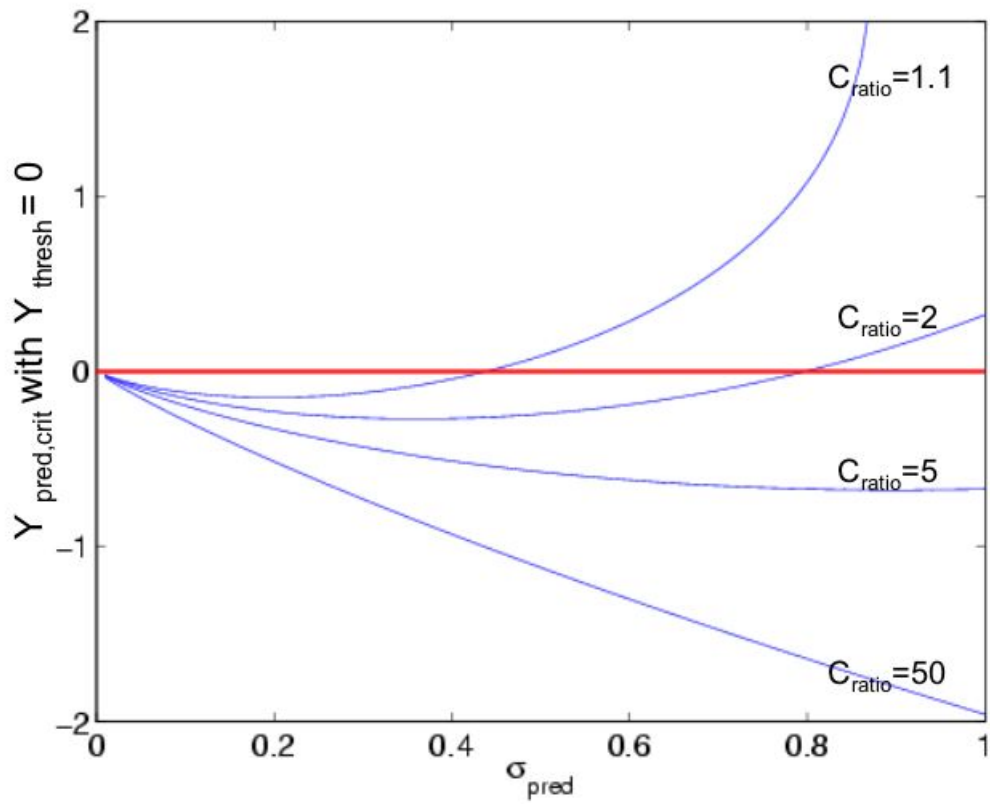


Figure 15

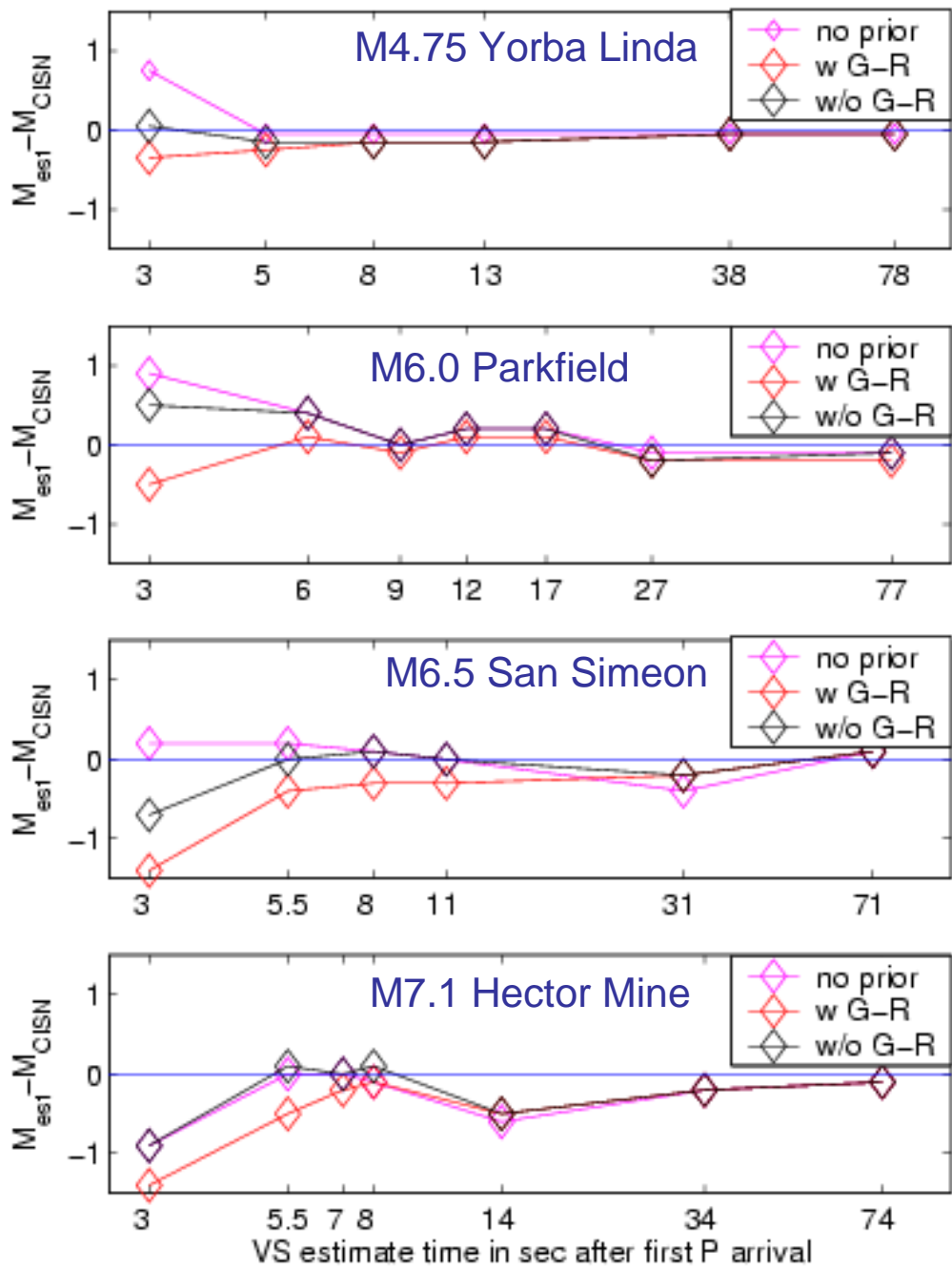


Figure 16